2020-01-01

Water Sourcing Strategies of Highly Resilient Vegetation in Desert Soils: Stable Isotope Analysis of a Northern Chihuahuan Desert Ecosystem

Hayden Eleanor Thompson
University of Texas at El Paso

WATER SOURCING STRATEGIES OF HIGHLY RESILIENT VEGETATION IN DESERT SOILS: STABLE ISOTOPE ANALYSIS OF A NORTHERN CHIHUAHUAN DESERT ECOSYSTEM

HAYDEN ELEANOR THOMPSON

Master's Program in Geological Sciences

APPROVED:

Hugo Gutiérrez-Jurado, Ph.D., Chair

Anthony Darrouzet-Nardi, Ph.D.

Lixin Jin Ph.D.

Lin Ma, Ph.D.

Stephen Crites, Ph.D.
Dean of the Graduate School

WATER SOURCING STRATEGIES OF HIGHLY RESILIENT VEGETATION IN DESERT SOILS: STABLE ISOTOPE ANALYSIS OF A NORTHERN CHIHUAHUAN DESERT ECOSYSTEM

by

HAYDEN ELEANOR THOMPSON, B.S.

THESIS

Presented to the Faculty of the Graduate School of

The University of Texas at El Paso

in Partial Fulfillment

of the Requirements

for the Degree of

MASTER OF SCIENCE

Department of Geological Sciences

THE UNIVERSITY OF TEXAS AT EL PASO

December 2020

Acknowledgements

Throughout the course of this thesis I have received guidance and assistance from numerous people for which I am thankful. Foremost, this research and subsequent thesis would not have been completed without the encouragement and support of my committee members. These important people provided invaluable advice, extensive knowledge, and endless patience throughout the duration of this project. I cannot thank you all enough.

I would like to extend my deepest gratitude to Orlando Ramirez-Valle and Amaris Bustamante. Orlando, te quiero agradecer por todo el tiempo que le haz dedicado a este estudio. Este proyecto no podria estar completo sin tu ayuda. Amaris, I cannot thank you enough for the numerous hours you devoted to helping me run samples, the beautiful sketches you created for my figures, your moral support, and most importantly, your friendship.

I would also like to extend my sincere thanks to Marguerite Mauritz-Tozer and Dr. Craig Tweedie with the Systems Ecology Laboratory at the University of Texas at El Paso. They provided me with meteorological data from their research in the Jornada that was instrumental for this thesis. Marguerite, I would like to especially thank you for your additional knowledge, guidance, and patience.

I want to thank Dr. Enrico Yepez at the Sonoran Institute of Technology for inviting us to use his laboratory and cryogenic vacuum extraction system for our vegetation samples. I would also like to thank him for his constructive feedback and insights on our isotopes data.

Additionally, I would like to thank the faculty and staff of the Department of Geological Sciences at UTEP that helped to guide and encourage me during this research. I would like to especially thank Annette Veilleux for tirelessly answering my questions, providing me with countless resources, and always offering moral support and positivity.

Finally, I would like to express my deepest appreciation to my family and friends for their never-ending love and support. Mom, I cannot thank you enough for always being there for me and providing me with continuous encouragement, positivity, and emotional support. Lynn, thank you for always cheering me up, being understanding, and providing me with your helpful insights, endless patience, and love.

Abstract

Plant water use strategies and water transport dynamics are important for understanding ecosystem productivity and soil-vegetation-atmosphere interactions within an environment (Li et al., 2007). Recent research using stable isotope analysis in wet and humid climates has found that vegetation uses tightly particle-bound water stored in the soil that does not participate in translatory flow (Brooks et al., 2010; Goldsmith et al., 2011; McDonnell 2014). In arid and semi-arid deserts of the United States, highly resilient vegetation, such as the Honey Mesquite (*Prosopis glandulosa*) and the Creosote shrub (*Larrea tridentata*), exhibit some degree of activity year-round despite limited water availability during the dry season. In an effort to determine the water sourcing strategies of these drought-tolerant species, as well as decern the existence and use of tightly bound soil water in arid and semi-arid environments, we collected and analyzed vegetation stems, soil, and precipitation samples from two sites over a 15-month period in the Jornada Experimental Range (JER) of the Northern Chihuahuan Desert.

Using stable isotopes of hydrogen (δ^2H) and oxygen ($\delta^{18}O$) we compared the isotopic composition of the mesquite and creosote xylem waters, to that of precipitation and soil water within the two study sites. One site was located in a low-lying channelized area (referred to as the Channel Area) and the other in a slightly higher, flatter area (referred to as the Flat Area). Our results indicate that the location of the vegetation and their associated soil in the landscape has an effect on the isotopic composition of the water they use. The soil water collected from the two study sites exhibited distinctly different behavior—soil water from the Channel Area would become enriched (or depleted) in ^{18}O and ^{2}H faster than the Flat Area. Vegetation stem water samples similarly exhibited different behaviors between the two sites. We found that creosote stem water samples followed the average behavior of the soil water at the site they were located in and

they had a larger range of $\delta^{18}O$ and $\delta^{2}H$ in both sites. This was an indication of their flexibility in arid and semi-arid environments—changing their source to take advantage of available resources (Reynolds et al., 1999; Peters and Gibbens, 2006). Consistent with previous studies, our results also revealed that precipitation and soil water samples from the JER have a seasonal variation in their isotopic composition that is linked to the location that the rainfall event was derived from (Wright et al., 2001; Hu and Dominguez, 2015). Our soil and precipitation samples were isotopically enriched in ^{18}O and ^{2}H during the summer, when rainfall is derived from the Gulf of Mexico, and they were depleted in ^{18}O and ^{2}H during the winter, when rainfall is derived from the Pacific Ocean. Lastly, our results displayed indications of the existence of tightly bound soil water and its possible use by mesquite and creosote within the JER. At the beginning of our study, the soil samples exhibited values that were extremely depleted in ^{18}O and ^{2}H and were not consistent with precipitation samples taken simultaneously. We suggest that a precipitation event with distinct values depleted in ^{18}O and ^{2}H could have occurred prior to our study and were tightly bound within the soil until a subsequent rainfall event. Patterns in the soil and vegetation stem water samples following this event indicate that large precipitation events at the beginning of each the monsoon and dry seasons supply moisture to the soil that is tightly bound and accessible to the vegetation when water is not readily available.

Table of Contents

Acknowledgements iv

Abstract vi

Table of Contents viii

List of Tables x

List of Figures xi

Chapter 1: Introduction 1

1.1 Problem 1

1.2 Flow of Water in the Subsurface 4

1.3 Isotopes as a Tracer of Vegetation Water Source 5

1.4 Significance 5

1.5 Objectives 6

Chapter 2: Methods 7

2.1 Study Area 7

2.2 Sample Collection 10

2.3 Meteorological and Soil Moisture Data 10

2.3 Stable Isotope Analysis 12

2.4 Cryogenic Vacuum Extraction 13

Chapter 3: Results 14

3.1 Hydrological Conditions During Study Period 14

3.1.1 Precipitation 14

3.1.2 Soil Moisture 15

3.1.3 Vapor Pressure Deficit 16

3.1.4 Evapotranspiration 17

3.2 Stable Isotopes 18

3.2.1 Precipitation 18

3.2.2 Soil Water 20

3.2.3 Vegetation Stem Water 25

3.3 Relationships Between Precipitation, Soil Water, and Vegetation Stem Water 29

3.3.1 Precipitation and Soil Water 29

3.3.2 Precipitation and Vegetation Stem Water 32
3.3.3 Soil Water and Vegetation Stem Water 33
Chapter 4: Discussion 35
4.1 Location Influence on Isotopic Composition 35
4.2 Variability of Isotopic Composition in Precipitation and Soil Water 37
4.3 Indications of Tightly Bound Soil Water 38
Chapter 5: Conclusions 40
5.1 Future Work 42
References 43
APPENDIX A: PROTOCOL FOR COLLECTING PRECIPITATION, STEM, AND SOIL SAMPLES FOR ISOTOPIC ANALYSIS WITH THE PICARRO L2130-I ANALYZER 48
APPENDIX B: PROTOCOL FOR ANALYZING STEM AND SOIL SAMPLES ON THE PICARRO L2130-I ANALYZER WITH AN INDUCTION MODULE 53
Vita 60

List of Tables

Table 1: Range of values for $\delta^{18}O$ and $\delta^{2}H$ in precipitation, vegetation, and soil samples. 30

List of Figures

Figure 1: Conceptual model of soil-vegetation-atmosphere interactions within the JER. 3
Figure 2: Area of interest. 7
Figure 3: Sampling locations. 9
Figure 4: SEL Tower in relation to sampling locations. 11
Figure 5: Daily precipitation and mean daily air temperature in JER during the study period. .. 14
Figure 6: Soil moisture (θ) and daily precipitation in the JER during the study period. 16
Figure 7: Mean daily VPD and daily precipitation in the JER during the study period. 17
Figure 8: (a) Daily and (b) cumulative ET and precipitation in the JER 18
Figure 9: Daily precipitation (mm) and $\delta^{18}O$ (‰) of precipitation samples 19
Figure 10: Global Meteoric Water Line (GMWL) vs. Local Meteoric Water Line (LMWL). .. 20
Figure 11: Plots of $\delta^{18}O$ vs $\delta^{2}H$ (‰) for soils and precipitation during the study period 21
Figure 12: Plots comparing the behavior of samples within the two sites (channel vs flat). 23
Figure 13: Plots comparing the behavior of samples within the two depths (10 cm vs 20 cm). . 24
Figure 14: Time series plot of $\delta^{18}O$ 26
Figure 15: Plots of $\delta^{18}O$ vs $\delta^{2}H$ (‰) for vegetation and precipitation during the study period. . 28
Figure 16: Box and whisker plots of $\delta^{18}O$ and $\delta^{2}H$ in soil, precipitation, and vegetation 31
Figure 17: Time series plots of precipitation and soil moisture 32
Figure 18: Time series plot of precipitation and vegetation collected during the study period. . 33
Figure 19: Time series plots of vegetation and soil 34
Figure 20: Plots of $\delta^{18}O$ vs $\delta^{2}H$ (‰) for vegetation and soil during the study period 34

Chapter 1: Introduction

1.1 Problem

In arid and semiarid ecosystems of the Northern Chihuahuan Desert, vegetation species such as Creosote (*Larrea tridentata*) and Honey Mesquite (*Prosopis glandulosa*) have the ability to maintain some degree of activity despite low shallow soil moisture conditions and high evaporative demand during the dry season. In high elevation regions of the Northern Chihuahuan Desert, away from perennial surface water sources (e.g. the Rio Grande), precipitation events and their associated runoff are the only source of surface water for these arid ecosystems. The activity of the Honey Mesquite and, particularly of the Creosote shrubs in these areas throughout the year, implies that these species have nearly continuous access to a source of water during the dry and largest part of the year (e.g. spring and late fall for both plants as well as winter for the Creosote). There are two possible explanations for this phenomenon: the plants are using their taproots to access deep soil water (>2m), or they are taking up tightly particle-bound soil water in the unsaturated zone from previous precipitation events.

Recent research in wet and temperate climates has found that some plants are using tightly bound soil water that is isotopically different than the water found in nearby streams and is thus not participating in translatory flow as previously believed (Brooks et al., 2010; Goldsmith et al., 2011; McDonnell 2014; Penna et al., 2013). This tightly bound soil water is produced through previous precipitation events and locked into small soil pores until taken up by the roots of plants during the dry season (Brooks et al., 2010). This compartmentalized ecohydrological system, known as the Two Water Worlds hypothesis, challenges the current translatory flow model in wet and temperate climates. In the translatory flow model, incoming rainfall displaces water previously in the soil horizons and pushes it further into the column, causing the oldest water at the bottom to

discharge into the aquifer. Little is known, however, about the occurrence of tightly bound soil water and its availability to plants within arid and semiarid ecosystems (Duniway et al., 2007; Duniway et al., 2009; Nobles et al., 2010).

Here we use stable isotopes of hydrogen (δ^2H) and oxygen ($\delta^{18}O$) to understand the temporal and spatial variability of plant source water use in semiarid and arid ecosystems. Our study focuses on Creosote and Honey Mesquite within the northern portion of the Chihuahuan Desert. The Chihuahuan Desert is the largest desert in North America with a total area of approximately 350,000 square kilometers (Schmidt 1979). We concentrate on Creosote and Honey Mesquite because they are two of the primary dominant species in the Northern Chihuahuan Desert since their grassland invasion around 1850 (Gibbens et al., 2005; Gile et al., 1998). They also have distinctly different root systems that could enable them to take-up water from separate soil horizons (Figure 1). Honey Mesquite can be phreatophytic with well-developed taproots that make them capable of reaching deep soil, and in some instances even groundwater, to overcome drought conditions (Ansley et at., 1990). Creosotes have shallow, laterally intermingled root systems that occur primarily within the top meter of soil (Gile et al., 1998). In addition, thick caliche soil layers can develop within the unsaturated zone of the Northern Chihuahuan Desert (Figure 1). Since caliche ($CaCO_3$) soil horizons are prevalent in most arid and semiarid environments—often within the rooting depths of many plant species—it can by hypothesized that they may affect the availability of plant-obtainable water in these areas (Duniway et al., 2007; Duniway et al., 2009).

This study looks at four Creosote and four Honey Mesquite plants from two sites within the Jornada Experimental Range (JER) of the Northern Chihuahuan Desert as an example of the conditions that could be expected in other arid and semiarid environments. I hypothesize that: (1) the isotopic signature of the Creosote and Mesquite xylem water will vary throughout the year

following the isotopic variability of the precipitation; (2) the isotopic signature of the soil water will vary with depth and time of year; and (3) the location of the plants and their associated soil within the landscape will affect their isotopic signature. The main hypothesis tested in this research is that the vegetation in these ecosystems are using tightly bound soil water stored in the unsaturated zone when water is not readily available to them from precipitation or runoff events.

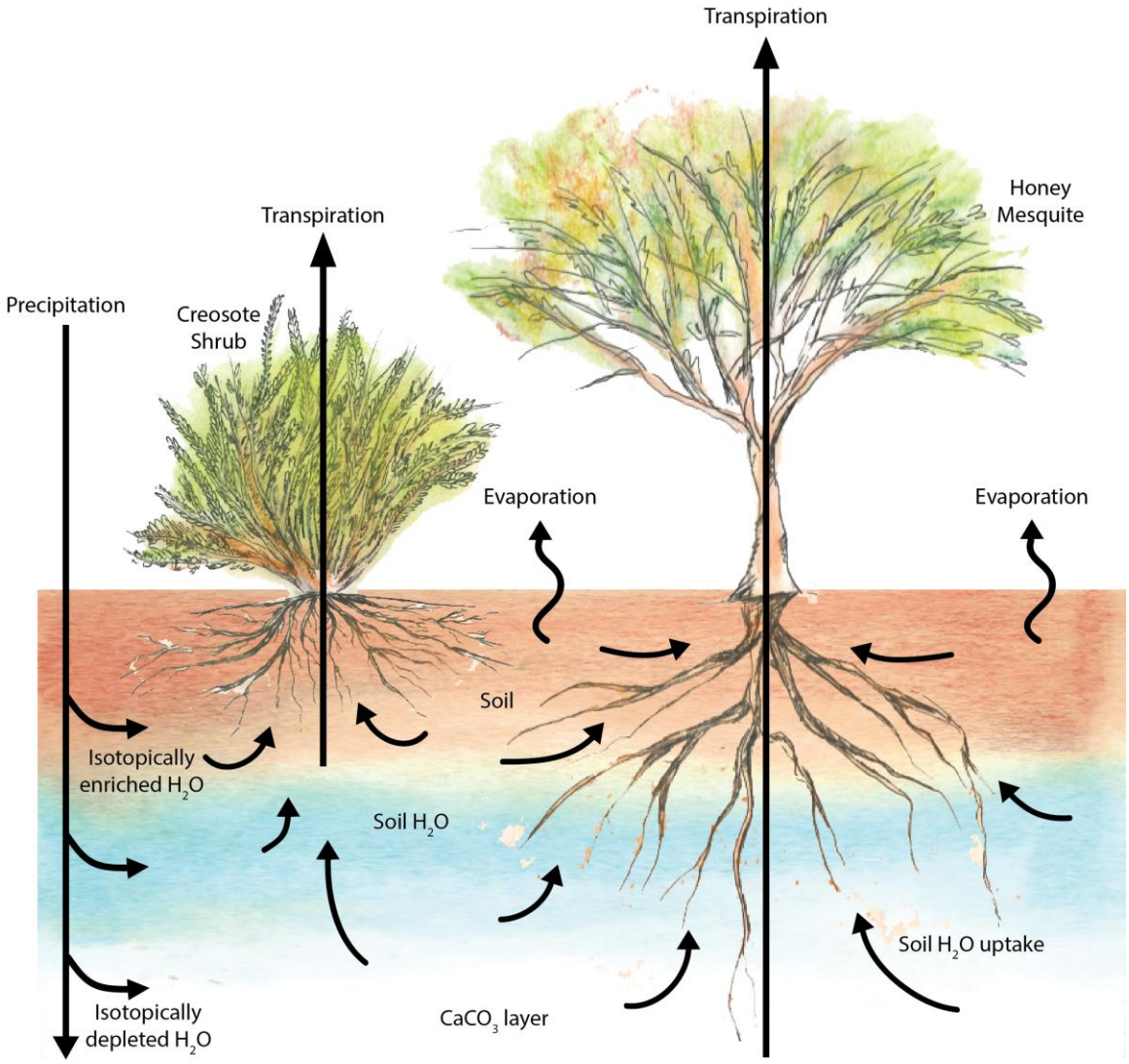

Figure 1: Conceptual model of soil-vegetation-atmosphere interactions within the JER. During the dry winter season (November – May), small, sporadic rainfall events provide isotopically depleted moisture to the soil. Temperature and ET are low, allowing most of the moisture to remain in the soil profile. During the monsoon season (June – October), larger precipitation events provide more isotopically enriched moisture to the soil. This water is either rapidly evaporated at shallow depths or mixes with any water previously in the soil. Creosotes and, to a lesser extent, mesquites shift their activity to take advantage of available water resources year-round. (Sketches by Amaris Bustamante, 2019)

1.2 Flow of Water in the Subsurface

Most hydrology models that evaluate water movement from the soil surface to the stream are commonly based on a translatory flow model with a single soil-moisture reservoir (Brooks et al., 2010; McDonnell 2014). In the translatory flow model, incoming precipitation pushes water present in the unsaturated soil zone from previous events deeper into the profile and eventually into the saturated zone that flows into a stream or aquifer. Water from multiple precipitation events is assumed to be well-mixed in a subsurface reservoir, and plants uptake the same water that ultimately goes into the streams (Brooks et al., 2010; McDonnell 2014). However, recent research has challenged this concept of translatory flow and proposed an alternate hypothesis based on a compartmentalized ecohydrological system; this has been called the "Two Water Worlds hypothesis" (McDonnell 2014).

In the Two Water Worlds hypothesis there are two separate systems: one immobile pool of water associated with vegetation transpiration and one mobile pool of water associated with stream replenishment or groundwater recharge (Brooks et al., 2010; Goldsmith et al., 2011; McDonnell 2014; Penna et al., 2013). Recent ecohydrological research discovered that tightly bound water is stored in the soil from the first precipitation event following the dry season. This tightly bound soil water does not participate in translatory flow. It is extracted by plants rather than being displaced by other precipitation events, mixing, and entering the stream. This leads vegetation to return different water to the hydrosphere than that of the stream (Brooks et al., 2010; Goldsmith et al., 2011; McDonnell 2014). In arid and semiarid environments, such as the Northern Chihuahuan Desert, these processes may be further affected by the presence of indurated caliche ($CaCO_3$) soil horizons that can restrict deep (>2m) water flow (Duniway et al., 2007; Duniway et al., 2009; Nobles et al., 2010) and high soil moisture evaporation rates (Gutiérrez-Jurado et al., 2006).

1.3 Isotopes as a Tracer of Vegetation Water Source

Hydrogen (δ^2H) and oxygen ($\delta^{18}O$) stable isotopes are increasingly being used as water source tracers for vegetation in ecosystems (Dawson and Ehleringer 1991; Goldsmith et al., 2011; Li et al., 2007; Penna et al., 2013). Because fractionation does not occur in hydrogen or oxygen during the uptake process by plant roots, the isotopic composition of the xylem water in plant stems can be assumed to resemble the isotopic composition of their source water (Li et al., 2007). A comparison of the hydrogen and oxygen isotopes in water from the surrounding environment to that of the plant xylem water can allow the determination of the plant's water most probable source (Dawson and Ehleringer 1991; Li et al., 2007). Some vegetation is thought to change water sources as a response to seasonal water availability (Li et al., 2007). Spatial and temporal variations of water uptake and water use by plants can therefore be traced using stable isotopes of water (δ^2H and $\delta^{18}O$). Additionally, water use patterns revealed by isotopic analysis can provide valuable information regarding the effects of vegetation productivity on hydrologic cycling in an ecosystem.

1.4 Significance

Plant water use strategies and water transport through soil-vegetation-atmosphere interactions are important for understanding basic desert ecosystem processes (Havstad et al., 2006). Understanding when and where these key desert plant species source their water in the Jornada Experimental Range (JER) will give us insight into biogeochemical cycling (Brooks et al., 2010), ecosystem productivity (Li et al., 2007), and nutrient transport (Brooks et al., 2010; McDonnell 2014) within the Chihuahuan Desert in particular, and other arid and semiarid environments where these plants occur as well (e.g. Sonoran and Mohave deserts). This will not only provide a foundation for advances in soil and hydrological modelling (Goldsmith et al., 2011; Li et al., 2007), it will also have significant implications for improving land management practices and conservation efforts in desert environments (Goldsmith et al., 2011; Havstad et al., 2006).

1.5 OBJECTIVES

This thesis presents isotopic data collected at the JER field site from November 2018 through January 2020. The main objectives of this study are to (a) determine if the topsoil (0-20 cm depth) above the caliche horizon holds a significant amount of soil water that is available for the plants to uptake year-round, (b) evaluate if and when the plants are changing their source of water throughout the year, (c) ascertain whether the location of plants in different landforms have an effect on the source of water they use, and (d) determine if the Two Water Worlds hypothesis pertains to arid/semiarid environments. By answering the questions implicit in the objectives, this study aims to determine the water sourcing strategies and patterns of water-use for the Honey Mesquite and Creosote shrubs throughout the year in the Jornada Experimental Range (JER) of the Northern Chihuahuan Desert.

Chapter 2: Methods

2.1 Study Area

The work presented in this thesis takes place in a shrub-dominated ecosystem within the U.S. Department of Agriculture-Agricultural Research Service (USDA-ARS) Jornada Experimental Range (JER) at the northern edge of the Chihuahuan Desert. The JER is located in south-central New Mexico, 30 km northeast of Las Cruces, within the Jornada Basin Long-Term Ecological Research (LTER) site (Figure 2). The Jornada Basin LTER is bordered by the Rio Grande Valley to the west and the San Andres Mountains to the east. Our research is conducted on a piedmont location of the JER in the vicinity of a large experimental array deployed and operated by the Systems Ecology Lab (SEL) at the University of Texas at El Paso for studying desert vegetation lifecycles and soil-vegetation-atmosphere gas exchanges. Samples were acquired from two sites within this region: Site 1 is located in a low-lying channelized area (32.5838 N, 106.633 W), while Site 2 is within a higher, flat area (32.5833 N, 106.632 W), approximately 60 to 90 meters apart (Figure 3).

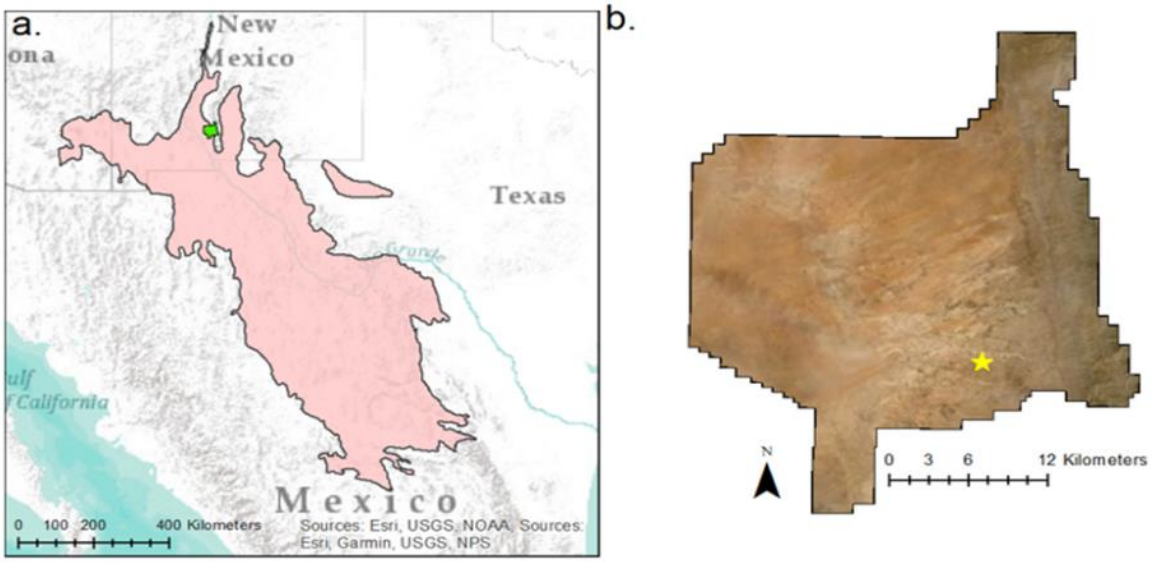

Figure 2: Area of interest. (a) Chihuahuan Desert (pink) and Jornada Experimental Range (green) in proximity to the United States and Mexico. (b) Map of Jornada Experimental Range with study area highlighted with yellow star.

The JER experiences long, hot summers with monsoonal precipitation and cool, predominantly dry winters. Average monthly air temperature ranges from 3.78°C in January to 26.03°C in July, with mean maximum temperatures ranging from 13.5°C in January to 34.96°C in July (Wainwright 2006; Ji et al., 2019). The JER receives an average of 245 mm/year of precipitation, with more than half deriving out of monsoonal storms in late summer (July through September), and the remainder from abbreviated precipitation events during the winter (December through February; Havstad et al., 2006). Summer rainfall accounts for approximately 64% of the annual precipitation and occurs as intense thunderstorms whose water sources can come from both the Pacific Ocean and the Gulf of Mexico (Ji et al., 2019; Peters and Eve, 1995; Wainwright 2006). Most winter moisture is derived from low intensity frontal storms from the Pacific Ocean (Ji et al., 2019; Peters and Eve, 1995; Wainwright 2006).

The Jornada Basin was previously covered in perennial grasses throughout the late 1800s and early 1900s; however, due to changing climate, overgrazing, and other factors, most of the area is now dominated by shrubs (Havstad et al., 2006; Reynolds et al., 2000). The Honey Mesquite (Prosopis glandulosa) and the Creosote Shrub (Larrea tridentata) are highly resilient desert shrubs that have become the dominant species in our two field sites in the JER (Figure 2; Ji et al., 2019; Peters and Eve, 1995). The spatial variability and maximum plant size of these species are governed by soil texture, topographic position, and water availability (Ji et al., 2019; Peters and Eve, 1995).

Figure 3: Sampling locations. Collection areas for soil and vegetation samples (green) and precipitation samples (blue) within the Jornada Experimental Range (JER). Site 1 is in the low-lying channelized area (32.5838 N, 106.633 W) and Site 2 is in the higher, flat area (32.5833 N, 106.632 W).

Our field sites in the JER contain piedmont slope alluvium derived from Paleozoic limestones and other associated clastic rocks (Monger et al., 2006). Sediments at the two sites have a gravelly sandy loam texture and are considered to be part of the Middle Tank Gravelly Soil Unit (Monger 2006). Sediments in the channel area (Site 1) are overlain and mixed with reddish-brown quartz sand deposits derived from the Ancestral Rio Grande (Monger et al., 2006). Both sites contain semi-indurated or indurated caliche ($CaCO_3$) soil horizons approximately 25 to 40 centimeters beneath the surface. Depth to the caliche varies between the two sites, with the caliche horizon in the flat area (Site 2) slightly deeper than in the channel area (Site 1). The caliche horizon is visible in some sections of the channel area (Site 1) where runoff has eroded small arroyos into the soil. The depth to groundwater near our study area is estimated to be greater than 75 meters (Monger et al., 2006) and likely unavailable to plants.

2.2 Sample Collection

Sampling was conducted approximately every two weeks between November 2018 and January 2020 in order to capture, as much as possible, the temporal variability in the isotopic values of precipitation, soil, and stem samples of the area. Precipitation was collected from two rainfall collectors installed into small pits, one on the University of Texas at El Paso (UTEP) campus (located approximately 90 km south of JER) and the other within the soil at the study area in JER. The rainfall collectors gathered precipitation from a funnel into a tube that was partially filled with mineral oil to avoid evaporation until the sample could be taken. The rainfall collector at JER was installed within 50 to 100 meters of the two study sites (Figure 3) to ensure that samples would be an accurate representation of the rainfall received by the ecosystem. The precipitation samples were collected at a variable interval—depending on the occurrence of a rainfall event. Additional meteorological data was collected from the SEL's weather gauges and the Jornada Rangeland Research Programs website (https://jornada.nmsu.edu/data-catalogs/weather-gauges). Vegetation stems were collected from a total of eight individual plants: two Mesquites and two Creosotes from each study site. One to three small pieces of stem were carefully cut from healthy branches of each of the plants using gardening shears. Soil samples were collected in glass jars at 10-centimeter and 20-centimeter depths from each site, taken in locations between the plants of interest in that area. All samples were wrapped in laboratory film (e.g. parafilm) and placed into a cooler with ice packs during transportation to the lab. In the lab, all samples were placed into the refrigerator until they could be analyzed. Detailed sample protocols and procedures regarding sample collection and handling can be found in Appendix A.

2.3 Meteorological and Soil Moisture Data

Precipitation, evapotranspiration (ET), temperature, vapor pressure deficit (VPD), and soil moisture (θ) data were obtained from the Systems Ecology Laboratory's (SEL) moisture and

meteorological instrument network in the JER. The SEL Tower is located at 32.581954 N, 106.635017 W, within 350 meters of the two study sites (Figure 4). ET fluxes were collected at a height of 5 meters using an Li-7500 CO_2/H_2O gas analyzer and a CSAT3 sonic anemometer. ET was measured as latent energy (LE) in Wm^2. Temperature (air temperature) was measured in degrees Celsius (°C) using a Vaisala HMP probe HMP45C, also at 5m height. VPD was calculated from the measured relative humidity (RH) and temperature using the fCalcVPDfromRHandTair function in the ReddyProc v1.2.2 package in R. Soil moisture was measured using Decagon Echo EC-5 moisture sensors installed horizontally at 5 cm, 10 cm, 20 cm, and 30 cm below four land-cover types. Soil moisture was measured as volumetric water content in m^3/m^3. Precipitation was measured in mm using a Texas tipping bucket rain gauge (TE525, Campbell Scientific).

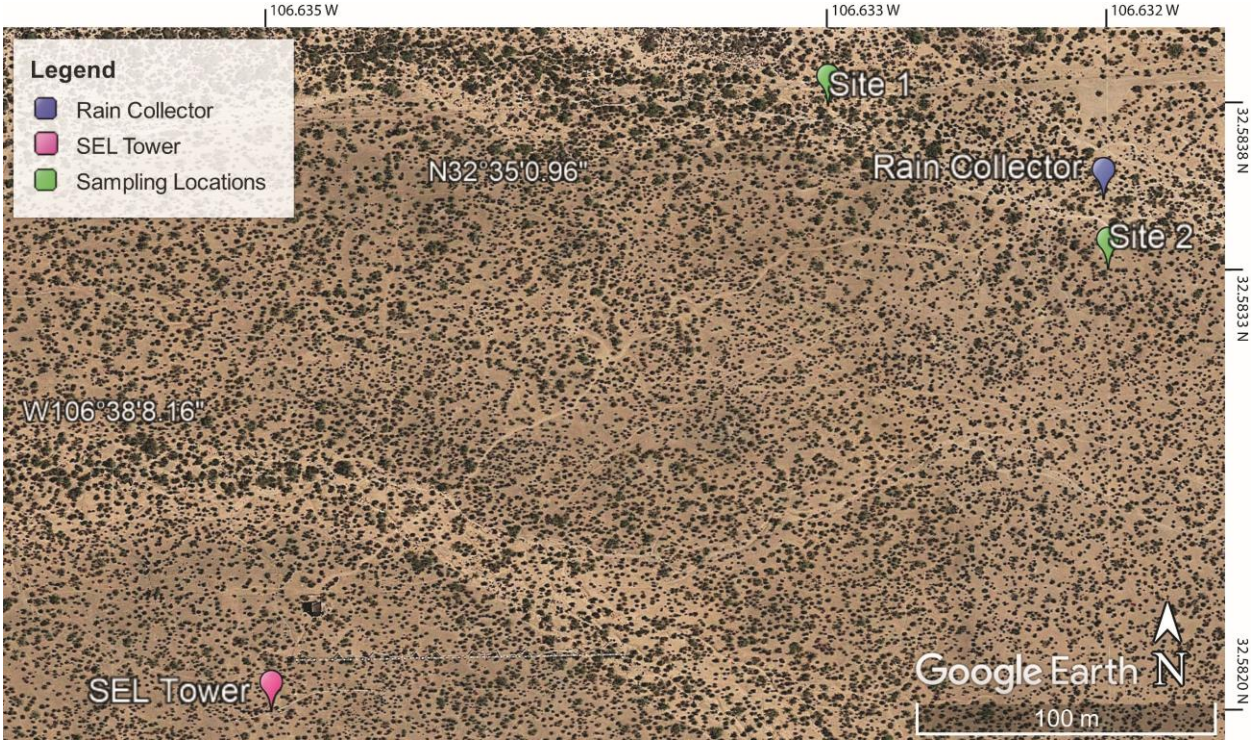

Figure 4: SEL Tower in relation to sampling locations. Systems Ecology Laboratory's (SEL) moisture and meteorological instrument network (pink), sample collection locations (green), and rainfall collector (blue) within the Jornada Experimental Range (JER). Site 1 is in the low-lying channelized area (32.5838 N, 106.633 W) and Site 2 is in the higher, flat area (32.5833 N, 106.632 W).

2.3 STABLE ISOTOPE ANALYSIS

Cavity ring-down spectroscopy (CRDS) was used to determine the hydrogen and oxygen isotopic signatures of the water in each of the collected samples of soil, vegetation, and precipitation. Each stem, soil, and precipitation sample were analyzed using a Picarro Inc. model L2130-i Isotope and Gas Concentration Analyzer. We utilized two peripheral attachments for the Picarro L2130-i to run our samples: an Induction Module (IM) and a Vaporizer set up with an Autosampler. Vegetation stems and soil samples were analyzed using the L2130-i in combination with the Picarro Induction Module (IM-CRDS). The Induction Module is used for extraction and isotopic analysis of matrix-bound water in solid samples (stems, leaves, soil, etc.) without elaborate laboratory-based sample preparation (Document Library: A0213 (Induction Module) Datasheet, 2013). From the vegetation stems collected in the JER, small ~2 mm slices were cut for analysis and directly placed into a metal 'envelope' sample holder. Similarly, the soil collected in the field was carefully scooped into small 3.3 to 5 mm metal tubes. These metal sample holders for vegetation and soil were each placed within a sealed glass vial (4mL) that is inserted into the IM-CRDS (Document Library: A0213 (Induction Module) Datasheet, 2013). The glass vial is pierced through a septa in the lid by a needle within the Induction Module. Once activated through the graphical user interface (GUI), an induction coil within the IM-CRDS heats the metal sample holder within the vial. As it is heated matrix-bound water is released as water vapor and fed directly through the needle into the CRDS for hydrogen (δ^2H) and oxygen ($\delta^{18}O$) isotopic analysis (Document Library: A0213 (Induction Module) Datasheet, 2013). See Appendix B for a detailed description of our soil and stem analysis protocol.

Precipitation samples were analyzed using the L2130-i in combination with the Picarro High Precision Vaporizer set up with an Autosampler. The Autosampler and Vaporizer is set up for highly accurate, automated isotopic analysis of liquid water samples (Document Library:

A0211 and A0325 (High Precision Vaporizer and Auto Sampler) Datasheet, 2014). From the precipitation samples collected in the JER, the water is filtered from the mineral oil using a syringe and placed into a small glass vial (2mL). After all samples are filtered, the vials of precipitation water can then be placed within the metal sample holder in the Autosampler (up to 105 samples at a time). Once set up and activated through the GUI, the Autosampler will use a syringe to mechanically take sample water and place it into the Vaporizer. Following vaporization, the gas is released into the chamber of the CRDS for hydrogen (δ^2H) and oxygen ($\delta^{18}O$) isotopic analysis. All isotopic signatures are expressed in the delta notation (δ) as the permil (‰) difference between the sample and the reference.

2.4 Cryogenic Vacuum Extraction

Due to the low water content of these plants and the presence of volatile organic compounds within the samples, we had to rerun a group of our vegetation samples by extracting water out of the plant stems using the cryogenic method. A cryogenic vacuum extraction system was used to extract water from mesquite and creosote samples taken between May 16, 2019 and January 24, 2020. Vegetation stem samples were cut into small pieces to facilitate water extraction and placed into tubes. These tubes were connected to a vacuum extraction unit and heated to ~100°C to evaporate the water. The water vapor that was created then begins to condense in a sample collector tube that was frozen using liquid nitrogen. This causes the water sample to freeze into a cryogenic "trap". Once defrosted, the samples were run in the Induction Module (IM) for hydrogen (δ^2H) and oxygen ($\delta^{18}O$) isotopic analysis. See Appendix B for a detailed description of our protocol for liquid sample analysis using the IM.

Chapter 3: Results

3.1 Hydrological Conditions During Study Period

3.1.1 Precipitation

This study spanned over a year of hydrological data in the Jornada Experimental Range (JER) from October 2018 to January 2020. Rainfall data during the study period from a nearby (<100m) set of meteorological instruments shows that precipitation is variable in the JER and can occur at any time of the year but has a seasonality similar to air temperature. Precipitation predominantly occurs from June through October when temperatures are at their highest for the year (Figure 5). As temperatures decrease in the winter months, precipitation events become smaller and more sporadic. The total precipitation during the study period was 410.89 mm of which 325.70 mm (79%) fell during the monsoon season (June – October) and 85.19 mm (21%) fell during the dry season (November – May). The largest amount of precipitation occurred on October 23, 2018, with a total of 52.84 mm of rain measured that day.

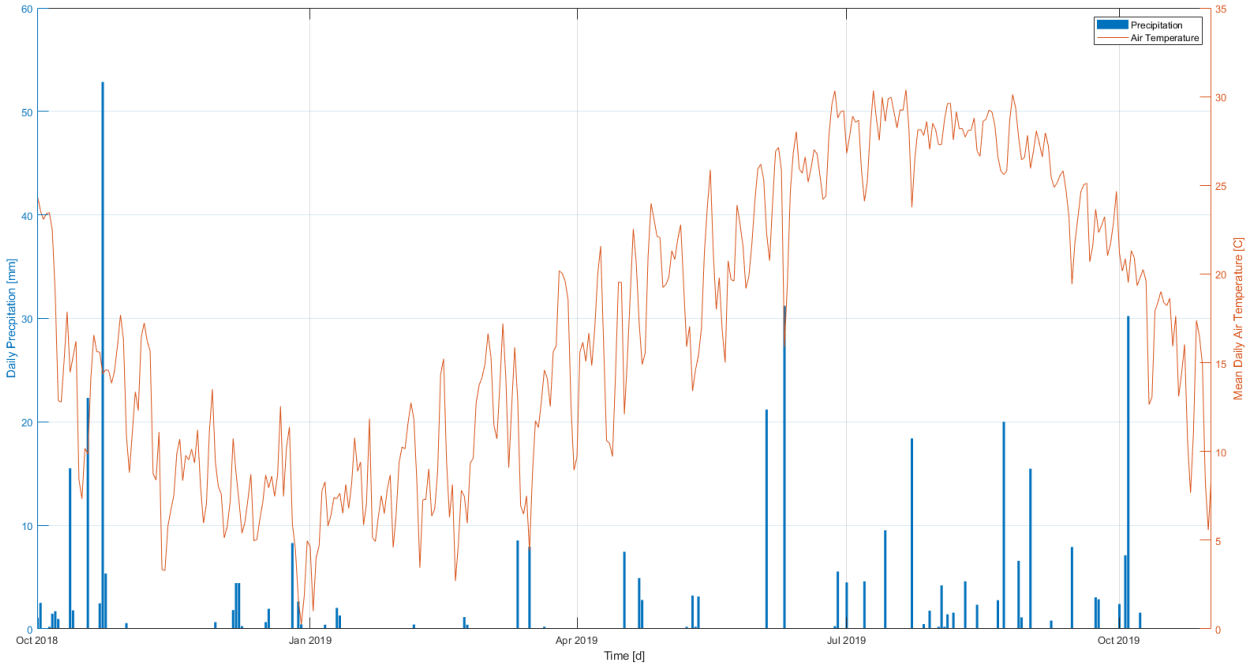

Figure 5: Daily precipitation and mean daily air temperature in JER during the study period. Measured by the Systems Ecology Laboratory's (SEL) weather gauges in the JER, located approximately 350 m from the study area.

3.1.2 Soil Moisture

This study used data collected by the SEL from three soil moisture sensors beneath a Creosote shrub at depths of 10 cm, 20 cm, and 30 cm. The soil moisture at these depths show a general pattern of wetting in response to large (>20 mm) precipitation events and drying between events (Figure 6). The soil at these depths appeared to have generally low ($\leq$0.1 $m^3\ m^{-3}$) soil moisture conditions throughout the year, aside from peaks in response to precipitation events. Generally, soil moisture at 10 cm increased the most in response to precipitation events, while soil moisture at 20 cm responded similarly with only a slight delay and soil moisture at 30 cm was moderately lagged and only responded to large (>30mm/d) precipitation events.

At the beginning of the study period there was a large rainfall event that caused the soil moisture at all depths to immediately increase to saturation, or partial saturation. This was followed by a slow recession of the moisture in the area—causing the moisture content in the soils to remain above 10% from October 2018 to March 2019. After this, moisture content in the soils continued to decay slowly through May 2019. The first monsoonal precipitation events occurred in June 2019 and moisture in the soil at depths of 10 cm and 20 cm immediately increased as a response. The monsoon season continued through October 2019, with moisture content in the soils, predominantly at 10 cm, increasing and decreasing in response to these events. Lastly, in the beginning of October there was another large rainfall event that immediately increased soil moisture content at 10 and 20 cm depths to partial saturation, and slowly receded to a value below 0.1 $m^3\ m^{-3}$ after two weeks.

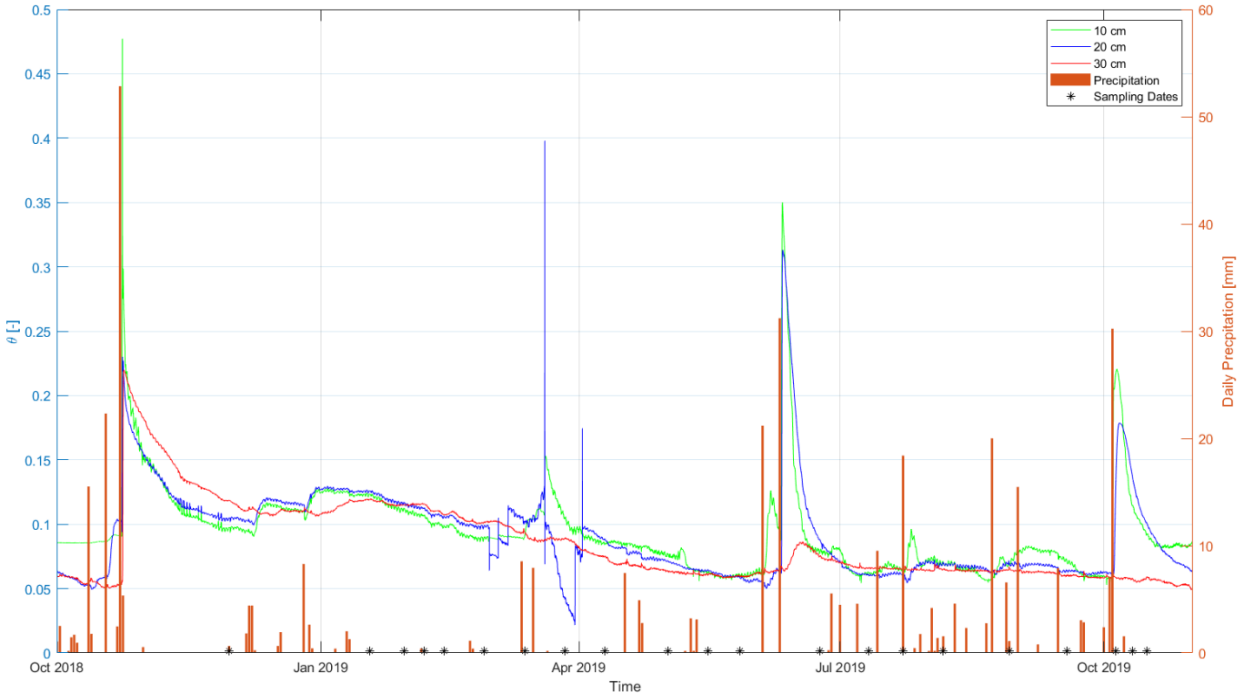

Figure 6: Soil moisture (θ) and daily precipitation in the JER during the study period. Data was provided by the Systems Ecology Laboratory's (SEL) moisture and meteorological instrument network in the JER, located approximately 350 m from the study area.

3.1.3 Vapor Pressure Deficit

Vapor pressure deficit (VPD) measured during the study period, although somewhat variable, shows a general seasonality with lower values during the winter months and higher values throughout the summer (Figure 7). In October 2018, part of the recessional limb of the high VPD season of 2018 (~April to October) occurs. Then, VPD remains low during the winter season from November to April. In late March 2019, the rising limb of the high VPD season of 2019 starts. The high VPD season runs from ~late April to October 2019. The VPD is higher in the summer because warmer temperatures raise the saturation vapor pressure while the humidity in the air remains low (average relative humidity from June to October 2019 was 33.76%). VPD is low during and immediately after precipitation events. In the winter when temperatures are low, VPD changes are slower than in the summer when temperatures are high. In the summer, the VPD only lowers briefly after large precipitation events and almost immediately returns to its previous value.

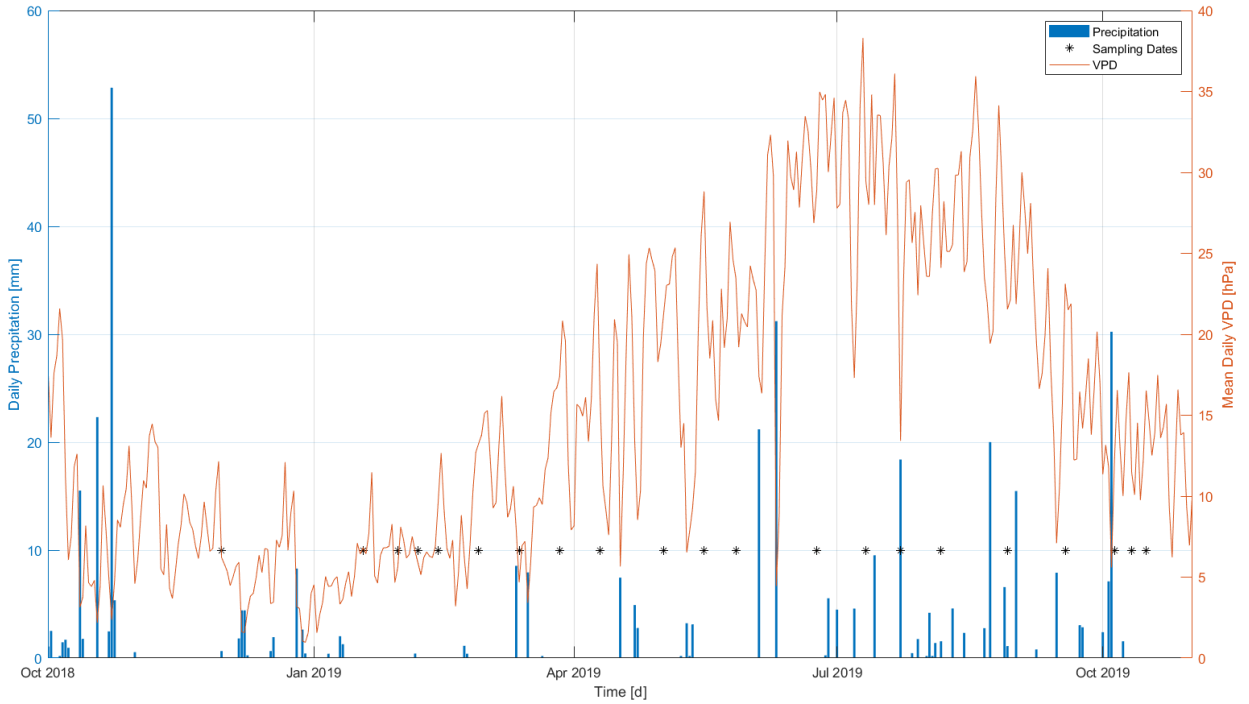

Figure 7: Mean daily VPD and daily precipitation in the JER during the study period. Measured by the Systems Ecology Laboratory's (SEL) weather gauges in the JER, located approximately 350 m from the study area.

3.1.4 Evapotranspiration

Evapotranspiration (ET) measured during the study period shows a general seasonality in response to precipitation and temperature: low ET values in the dry winter and higher values during the wetter summer months. In October 2018, the recessional limb of the high ET season (~June to October) occurred. This was followed by a dry period during the winter (November to March) where ET was low, and precipitation only occurred sporadically. Larger precipitation events started occurring in the spring (~late March and April) when the rising limb of the 2019 ET peak season began. The main ET season ran from June to October in 2019. ET increased immediately following precipitation events. Cumulative precipitation is greater than cumulative ET during the study period (Figure 8). This means some water from precipitation events is either leaving the system through surface runoff or staying in the system as storage into the soil.

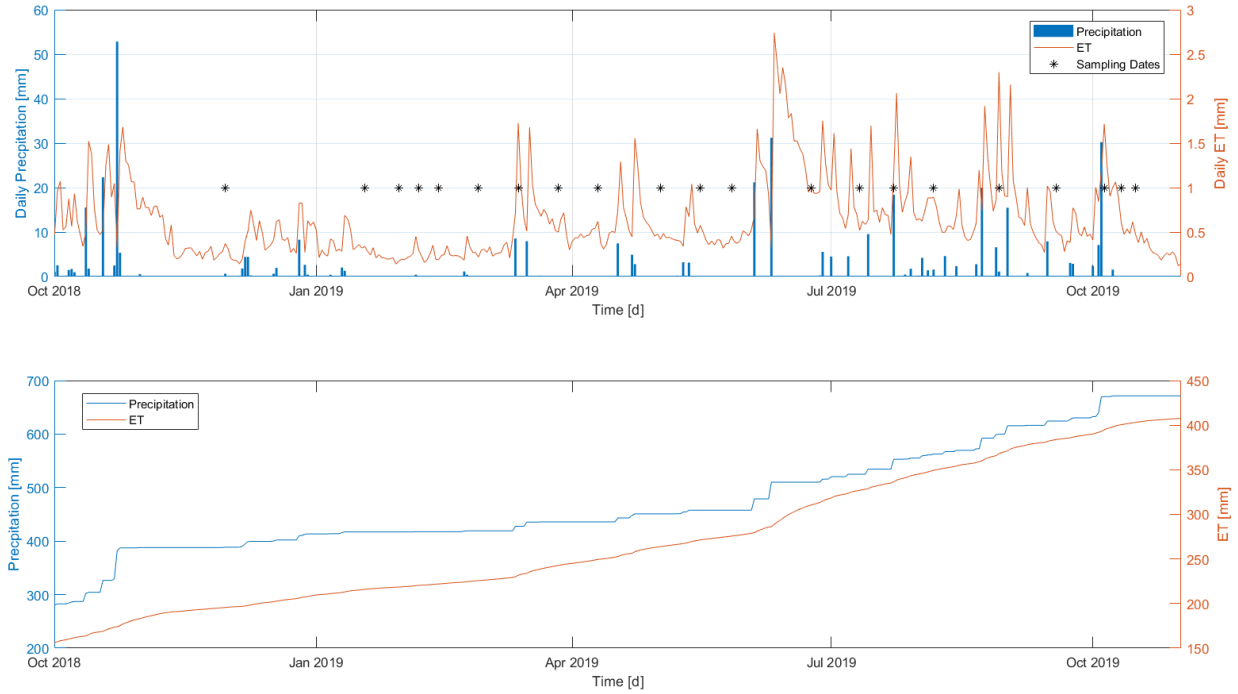

Figure 8: (a) Daily and (b) cumulative ET and precipitation in the JER during the study period. Daily ET is compared to daily precipitation in the top graph, while cumulative ET is compared to cumulative precipitation in the bottom graph. Measured by the Systems Ecology Laboratory's (SEL) weather gauges in the JER, located approximately 350 m from the study area.

3.2 Stable Isotopes

3.2.1 Precipitation

There was a total of 35 precipitation samples collected for isotopic analysis during the study period: 21 samples from the rainfall collector at UTEP and 14 from the rainfall collector in JER (Figure 9). At the beginning of the study period, $\delta^{18}O$ of precipitation was depleted in ^{18}O (~ -11 ‰) and remained relatively depleted until March 2019. As the year progressed into summer, precipitation $\delta^{18}O$ generally became more enriched in ^{18}O and eventually peaked in late August (~ 11 ‰). Following this peak, precipitation $\delta^{18}O$ immediately decreased to ~ -5 ‰. The values rose again slightly in September and then slowly became more depleted in ^{18}O as the year transitioned into winter, dipping to values as low as ~ -17 ‰. At the beginning of January 2020, $\delta^{18}O$ of precipitation began to increase again, rising to ~ -3 ‰ at the end of the study period. There is some variability in the oxygen isotopes over this time: the values range from more depleted or enriched

in ^{18}O responding to precipitation events and their associated periods of evaporation—ultimately depending on the time in which the sample was collected following a rainfall event.

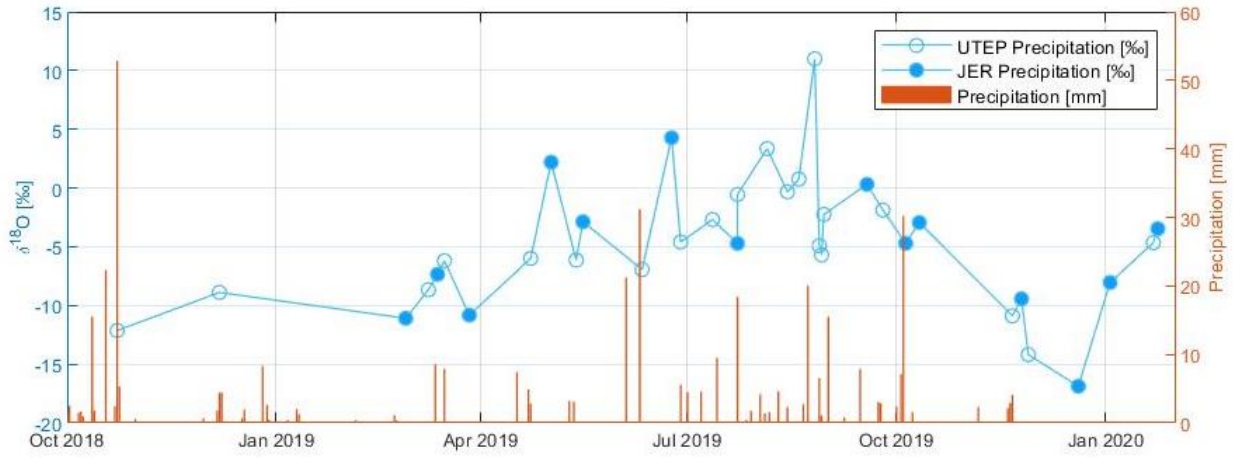

Figure 9: Daily precipitation (mm) and $\delta^{18}O$ (‰) of precipitation samples collected during the study period. Blue circles represent the $\delta^{18}O$ of precipitation samples collected from the two rainfall collectors: open circles are from the UTEP campus and filled circles are from the JER. Daily precipitation (mm), depicted by orange bars, was measured by the Systems Ecology Laboratory's (SEL) weather gauges in the JER, located approximately 350 m from the study area.

The $\delta^{18}O$ of precipitation ranged from -16.88 ‰ to 11.00 ‰ during the study period with an average $\delta^{18}O$ of -4.80 ‰ (Table 1). The $\delta^{2}H$ of precipitation ranged from -134.17 ‰ to 37.36 ‰ throughout the study period with an average value of -38.84 ‰. The monsoon season (June-October) had an average $\delta^{18}O$ of -1.32 ‰ and an average $\delta^{2}H$ of -11.92 ‰, while the drier season (November-May) had average values of -8.08 ‰ and -64.27 ‰, respectively. The Global Meteoric Water Line (GMWL), following Harmon Craig (1961), is $\delta^{2}H = 8.0*\delta^{18}O+10‰$. The Local Meteoric Water Line (LMWL), obtained from our precipitation samples, is $\delta^{2}H = 6.3*\delta^{18}O-8.7‰$. The differences between the LMWL and GMWL can be attributed to the contrasting size of the data sets and the locality of our samples collected for the LMWL (Figure 10).

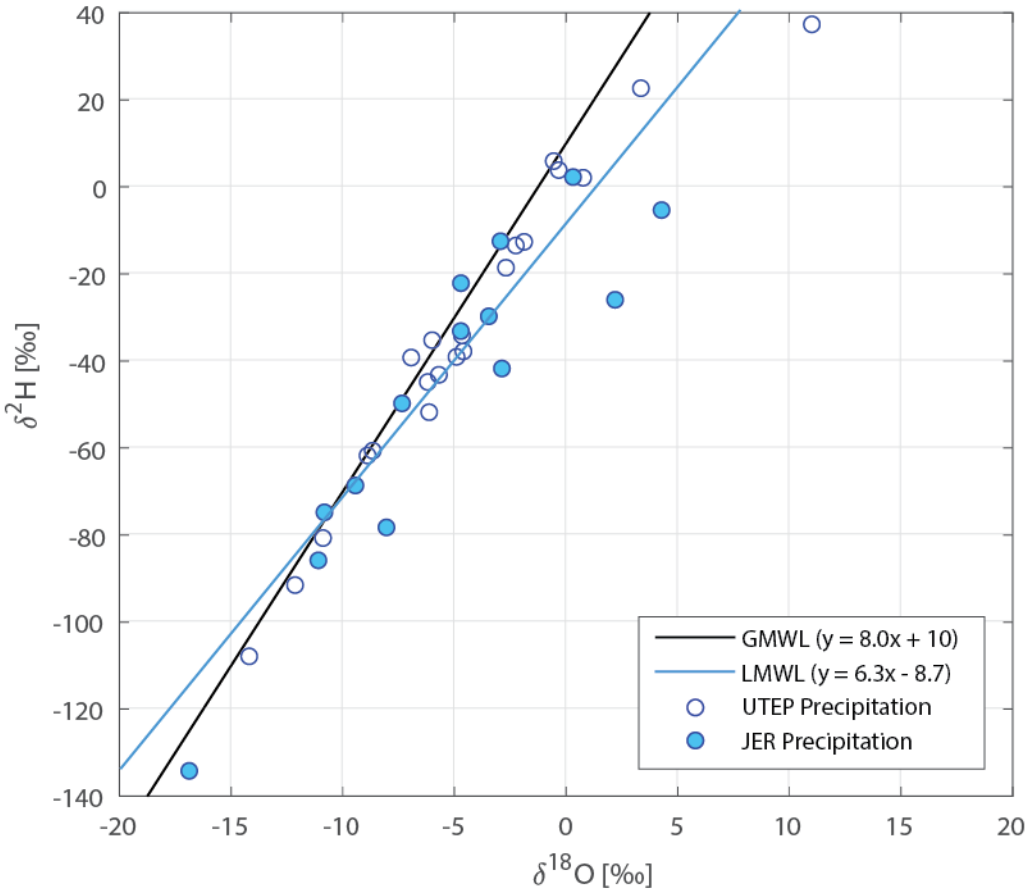

Figure 10: Global Meteoric Water Line (GMWL) vs. Local Meteoric Water Line (LMWL). Open circles are from the UTEP campus and filled circles are from the JER.

3.2.2 Soil Water

The $\delta^{18}O$ of soil collected at 10 centimeters ranged from -17.32 ‰ to 4.77 ‰ during the study period with an average $\delta^{18}O$ of -5.32 ‰ (Table 1). The $\delta^{2}H$ of 10-centimeter soil ranged from -89.49 ‰ to -9.87 ‰ throughout the study period with an average value of -49.67 ‰. Soil collected at 20 centimeters had $\delta^{18}O$ ranging from -16.97 ‰ to 5.28 ‰ with an average $\delta^{18}O$ of -6.76 ‰. The $\delta^{2}H$ of 20-centimeter soil ranged from -96.89 ‰ to -7.90 ‰ with an average value of -51.18 ‰. Soils collected in the channelized area (Site 1) have an average $\delta^{18}O$ of -6.79 ‰ and an average $\delta^{2}H$ of -52.93 ‰, while the flat area (Site 2) had average values of -5.29 ‰ and -47.93 ‰, respectively.

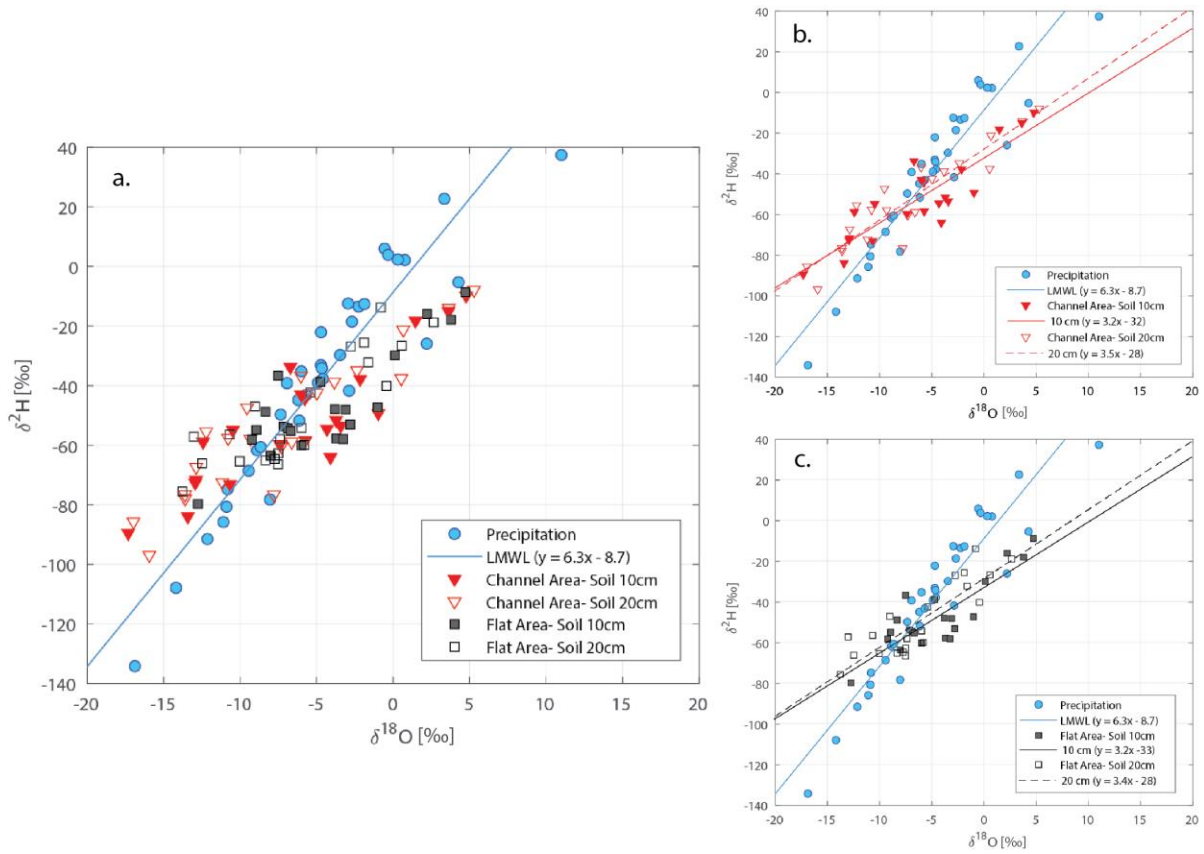

Figure 11: Plots of $\delta^{18}O$ vs $\delta^{2}H$ (‰) for soils and precipitation during the study period. (a) Precipitation samples plotted with soil collected at 10 and 20 cm in both study areas. (b) Soil samples collected at 10 and 20 cm from the channel area (Site 1) with their linear regressions. (c) Soil samples collected at 10 and 20 cm from the flat area (Site 2) with their linear regressions. Red triangles denote soil samples collected in the channel area, black squares denote soil samples collected in the flat area, and blue circles denote precipitation samples. The LMWL is plotted for comparison.

Soils collected in the channelized area (Site 1) have similar isotopic signatures to the soils collected in the flat area (Site 2) with most of their values plotting between -10 ‰ to 0 ‰ $\delta^{18}O$ and -30 ‰ to -70 ‰ $\delta^{2}H$ (Figure 11). There are values that plot outside of this range in both of the study sites. However, there are more soils collected from the channelized area that plot below -10 ‰ $\delta^{18}O$ and -70 ‰ $\delta^{2}H$, whereas more soils collected from the flat area plot above 0 ‰ $\delta^{18}O$ and -30 ‰ $\delta^{2}H$. The soils from both study sites plot along the LMWL, with some values both more depleted in ^{18}O and ^{2}H and some more enriched in ^{18}O and ^{2}H than the local precipitation.

The linear regressions for each depth of soil collected at the two study sites was plotted in Figure 11. In the channelized area the linear regression of the 10 cm soil samples is slightly enriched in ^{18}O and ^{2}H (y = 3.19*x -32.4) in comparison to that of the samples collected at 20 cm (y = 3.49*x – 27.9). Similarly, in the flat area the samples collected at 10 cm are slightly more enriched in ^{18}O and ^{2}H (y = 3.22*x -32.8) than that of the 20 cm samples (y = 3.39*x -28). The two linear regressions for the flat area samples are more similar (slopes are 0.17 different) than the regressions for the channelized area (slopes are 0.30 different).

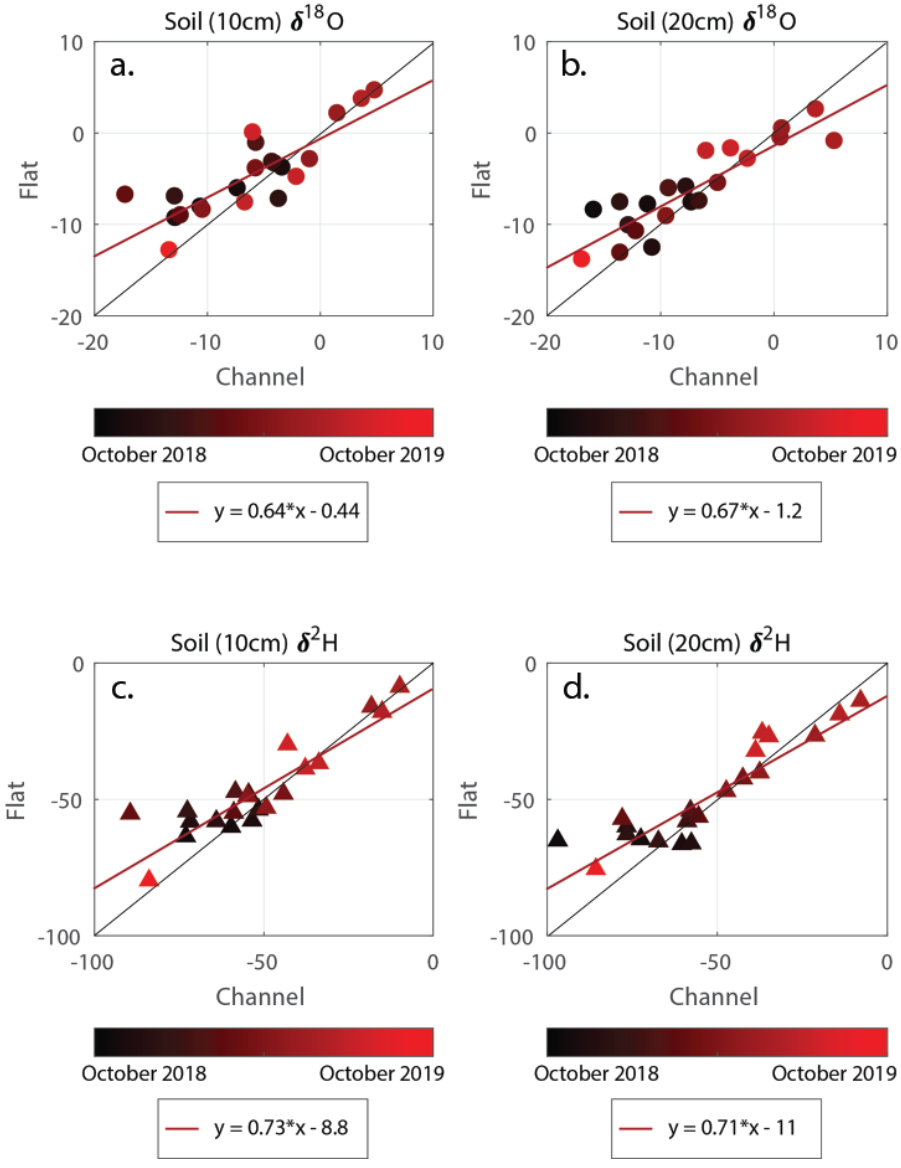

Figure 12: Plots comparing the behavior of samples within the two sites (channel vs flat). (a) $\delta^{18}O$ (‰) from soil samples collected at 10 cm. (b) $\delta^{18}O$ (‰) from soil samples collected at 20 cm. (c) $\delta^{2}H$ (‰) from soil samples collected at 10 cm. (d) $\delta^{2}H$ (‰) from soil samples collected at 20 cm. Samples are colored in accordance with their collection date. Red lines denote the linear trend of the samples. Black lines denoted a one-to-one linear relationship for comparison.

To assess the differences in the soil water isotopes behavior between sites for each soil depth sample, $\delta^{18}O$ and $\delta^{2}H$ of the channel area were plotted against those of the flat area. The results show that the samples collected in the channelized area have $\delta^{18}O$ and $\delta^{2}H$ values similar to those collected in the flat area. However, when comparing the range of values between flat and channel soils expressed in the slope of the data fittings, it is clear that samples in the channelized area become more enriched (show a wider range) or depleted in ^{18}O and ^{2}H faster than the samples in the flat area (Figure 12). This trend can be seen in both sample collection depths (10 cm and 20 cm), as well as, in both $\delta^{18}O$ and $\delta^{2}H$. When assessing how the samples in the two areas behave over the duration of the study period it becomes apparent that they have a seasonal trend. The samples are generally depleted in ^{18}O and ^{2}H at the beginning of the study (October 2018; black or dark red symbols in Figure 12) and become more enriched in ^{18}O and ^{2}H into the summer months, then start to become depleted again towards the end of the study (October 2019; bright red symbols in Figure 12).

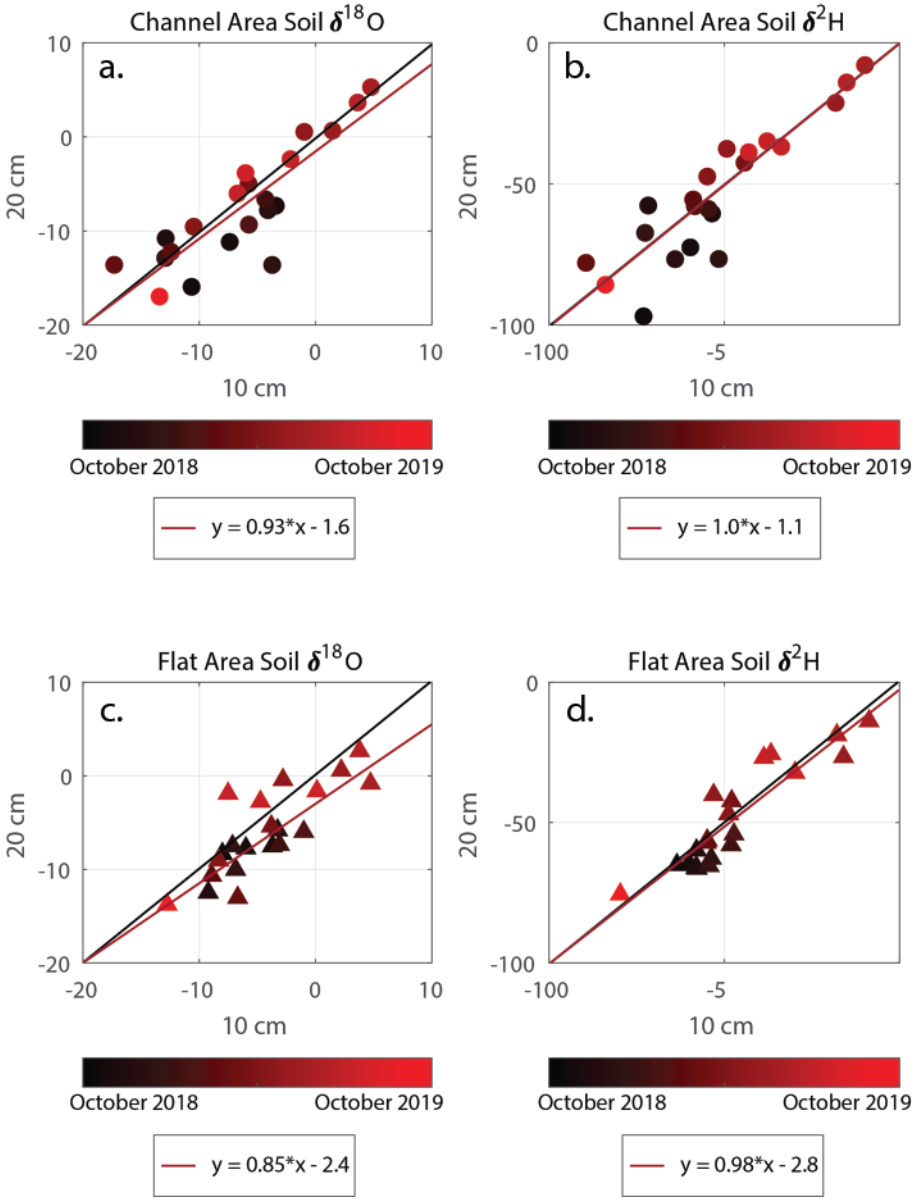

Figure 13: Plots comparing the behavior of samples within the two depths (10 cm vs 20 cm). (a) $\delta^{18}O$ (‰) from soil samples collected in the channel area. (b) $\delta^{2}H$ (‰) from soil samples collected in the channel area. (c) $\delta^{18}O$ (‰) from soil samples collected in the flat area. (d) $\delta^{2}H$ (‰) from soil samples collected in the flat area. Samples are colored in accordance with their collection date. Red lines denote the linear trend of the samples. Black lines denoted a one-to-one linear relationship for comparison.

When assessing the behavior of samples collected at the two depths, it becomes apparent that, in most cases, the samples collected at 10 cm become more enriched or depleted in ^{18}O and ^{2}H slightly faster than the samples collected at 20 cm (Figure 13). This trend can be seen in both the $\delta^{18}O$ and $\delta^{2}H$ of the flat area samples, as well as the $\delta^{18}O$ of the channel samples. However,

the δ^2H of the channel area samples shows a one-to-one linear relationship. There is also a seasonal trend in how the samples behave over the duration of the study. At the beginning of the study (October 2018; black or dark red symbols in Figure 13) the samples are depleted in ^{18}O and ^{2}H. As the year progresses into the summer the samples become increasingly more enriched in ^{18}O and ^{2}H. Then, towards the end of the study (October 2019; bright red symbols in Figure 13) the samples begin to be more depleted in ^{18}O and ^{2}H again.

3.2.3 Vegetation Stem Water

Although mesquite and creosote samples were originally collected from November 2018 to January 2020, only samples taken on or after May 17, 2019 were viable for cryogenic vacuum extraction. There are additional gaps in the data when a sample was not able to be cryogenically extracted due to low water content. The following results are from the viable vegetation stem water samples that were collected between May 2019 and January 2020.

From May to September 2019, $\delta^{18}O$ of mesquite and creosote were relatively depleted in ^{18}O and steadily ranged from ~ -5 ‰ to ~ 5 ‰ (Figure 14). During this time, the $\delta^{18}O$ of mesquite and creosote from both the channel and flat areas plot fairly close to each other, and some even overlap. However, from September 2019 to January 2020, the values become much more sporadic: rapidly changing from depleted in ^{18}O to enriched, then enriched in ^{18}O to depleted, and sometimes back to enriched again, each time they were sampled. During this second half of the year, $\delta^{18}O$ of mesquite and creosote ranged from ~ -7 ‰ to ~ 18 ‰. The $\delta^{18}O$ of mesquite and creosote generally plot separately from each other during this time.

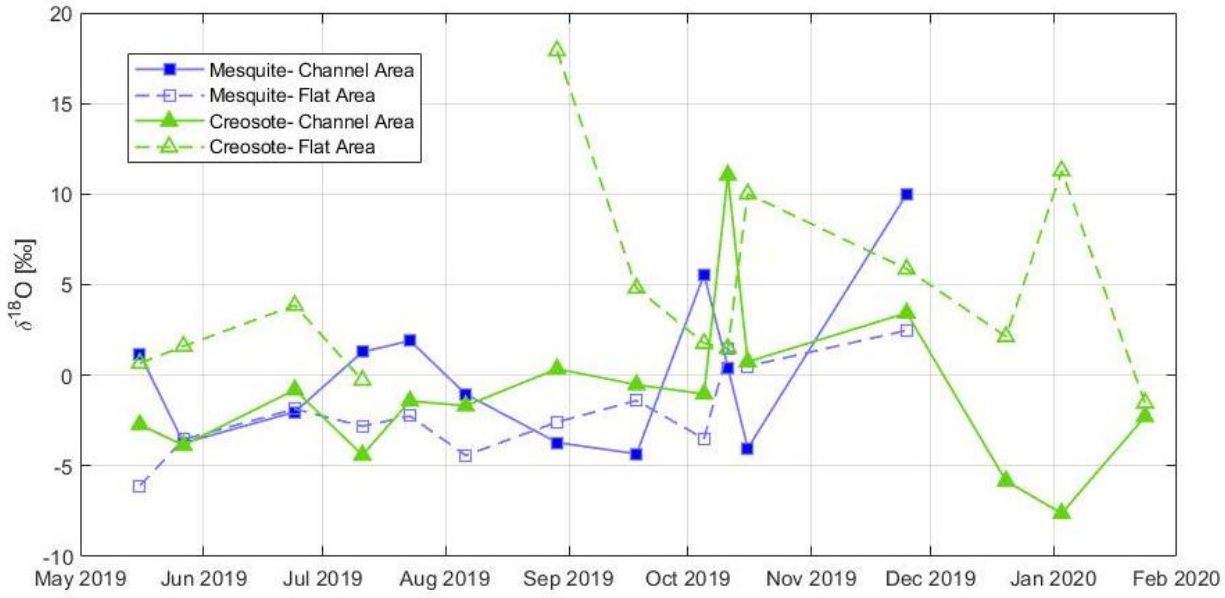

Figure 14: Time series plot of $\delta^{18}O$ (‰) of vegetation samples during the study period. Blue squares represent the $\delta^{18}O$ of mesquite samples collected from the two study areas. Green triangles represent the $\delta^{18}O$ of creosote samples collected from the two study areas. Filled symbols are collected from the channel area (Site 1) and empty symbols are collected from the flat area (Site 2).

The $\delta^{18}O$ of mesquite samples collected from the channel area ranged from -4.34 ‰ to 9.99 ‰ during the study period with an average $\delta^{18}O$ of 0.12 ‰ (Table 1). The $\delta^{2}H$ of channel area mesquite samples ranged from -57.26 ‰ to 4.69 ‰ throughout the study period with an average value of -40.28 ‰. Mesquite samples collected in the flat area had $\delta^{18}O$ ranging from -6.09 ‰ to 2.48 ‰ with an average $\delta^{18}O$ of -2.00 ‰. The $\delta^{2}H$ of flat area mesquite samples ranged from -70.19 ‰ to -40.17 ‰ with an average value of -56.50 ‰. Mesquite samples collected from both sites altogether have an average $\delta^{18}O$ of -0.94 ‰ and an average $\delta^{2}H$ of -48.39 ‰.

The $\delta^{18}O$ of creosote samples collected from the channel area ranged from -7.62 ‰ to 11.05 ‰ during the study period with an average $\delta^{18}O$ of -1.11 ‰ (Table 1). The $\delta^{2}H$ of channel area creosote samples ranged from -85.36 ‰ to -20.39 ‰ throughout the study period with an average value of -52.63 ‰. Creosote samples collected in the flat area had $\delta^{18}O$ ranging from -1.53 ‰ to 17.91 ‰ with an average $\delta^{18}O$ of 4.59 ‰. The $\delta^{2}H$ of flat area creosote samples ranged

from -61.65 ‰ to 13.50 ‰ with an average value of -31.07 ‰. Creosote samples collected from both sites altogether have an average $\delta^{18}O$ of 1.74 ‰ and an average $\delta^{2}H$ of -41.85 ‰.

The $\delta^{18}O$ and $\delta^{2}H$ ranges of mesquite and creosote samples collected from the channel (Site 1) and flat (Site 2) areas overlap (Figure 17 and Table 1). However, the $\delta^{18}O$ and $\delta^{2}H$ ranges of creosote samples collected from the flat area are significantly more enriched in ^{18}O and ^{2}H than that of creosote collected in the channel area and mesquite collected in both study areas. The $\delta^{18}O$ and $\delta^{2}H$ ranges of channel area creosote samples is more similar to that of the channel and flat area mesquite samples. When comparing the $\delta^{18}O$ and $\delta^{2}H$ averages of the two study areas, the vegetation from the flat area contains values that are both the most enriched in ^{18}O and ^{2}H (creosote: 4.59 ‰ and -31.07 ‰, respectively) and most depleted in ^{18}O and ^{2}H (mesquite: -2.00 ‰ and -56.50 ‰, respectively). However, when comparing the two types of plants, the creosote samples altogether have a larger range of $\delta^{18}O$ and $\delta^{2}H$ (-7.62 to 17.91 ‰ in $\delta^{18}O$ and -85.36 to 13.50 ‰ in $\delta^{2}H$) that encompasses the range of that in the mesquite samples (Figures 14 and 17).

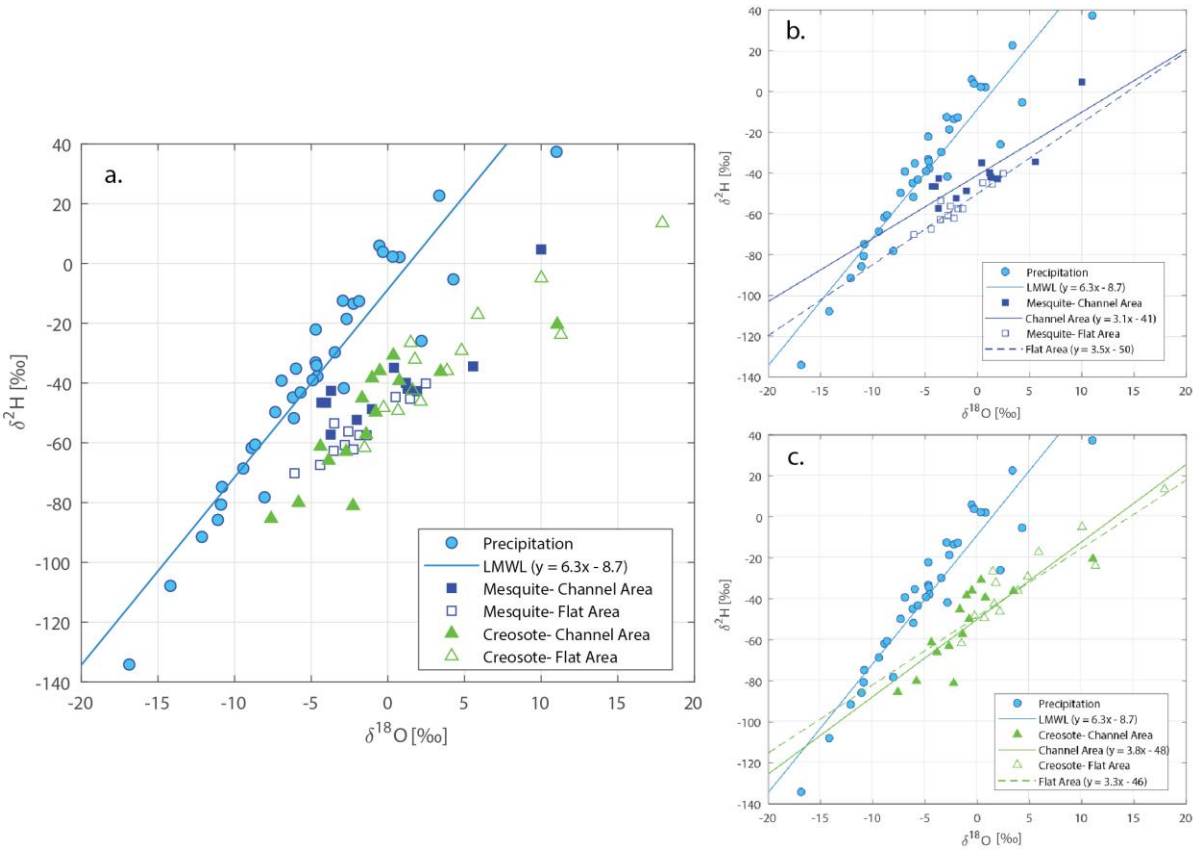

Figure 15: Plots of $\delta^{18}O$ vs $\delta^{2}H$ (‰) for vegetation and precipitation during the study period. (a) Precipitation samples plotted with mesquite and creosote samples collected from both the channel (Site 1) and flat (Site 2) areas. (b) Mesquite samples with their linear regressions. (c) Creosote samples with their linear regressions. Blue squares denote mesquite samples, green triangles denote creosote samples, and blue circles denote precipitation samples. Filled symbols are collected from the channel area (Site 1) and empty symbols are collected from the flat area (Site 2). The LMWL is plotted for comparison.

Vegetation samples collected in the channelized area (Site 1) have similar isotopic signatures to the samples collected in the flat area (Site 2), with the majority of their values plotting between -5 ‰ to 5 ‰ $\delta^{18}O$ and -30 ‰ to -70 ‰ $\delta^{2}H$ (Figure 15). However, there are mesquite and creosote samples that plot outside of this range in both of the study areas. In the channel area, creosote samples are distinctly more depleted in ^{18}O and ^{2}H than the mesquite samples. Whereas, in the flat area the mesquite samples are more depleted in ^{18}O and ^{2}H than the creosote samples. When assessing the plants individually, the mesquite samples have a much smaller range of values than that of the creosote samples. The vegetation samples collected from both sites plot next to the

LMWL, only overlapping slightly with the values of precipitation that are more enriched in ^{18}O and ^{2}H.

The linear regressions for each plant in the two study sites are graphed in Figure 15. The vegetation samples collected in the flat area are more enriched in ^{18}O and ^{2}H than the samples collected in the channel area. In the flat area, the linear regression of creosote samples is only slightly more enriched in ^{18}O and ^{2}H ($y = 3.3*x - 46$) than the mesquite samples ($y = 3.5*x - 50$). However, in the channel area, the linear regression of mesquite samples is more enriched in ^{18}O and ^{2}H ($y = 3.1*x - 41$) than the creosote samples ($y = 3.8*x - 48$). The two linear regressions for the flat area samples are more similar (slopes are 0.2 different) than the regressions for the channelized area (slopes are 0.7 different). Looking closer, the two linear regressions for the mesquite samples altogether are more similar (slopes are 0.4 different) than the regressions for all of the creosote samples (slopes are 0.5 different).

3.3 Relationships Between Precipitation, Soil Water, and Vegetation Stem Water

3.3.1 Precipitation and Soil Water

The $\delta^{18}O$ and $\delta^{2}H$ ranges of precipitation and soil water overlap (Figure 16). However, the average $\delta^{18}O$ and $\delta^{2}H$ of soil water samples are generally more depleted in ^{18}O and ^{2}H than that of precipitation samples (Table 1). The soil samples collected at 10 cm in both the channelized area (Site 1) and the flat area (Site 2) are, on average, more enriched in ^{18}O and ^{2}H than those collected at 20 cm. When comparing the two sites, the channelized area has both values more enriched in ^{18}O and ^{2}H and more depleted in ^{18}O and ^{2}H than the flat area. However, the channelized area on average, is more enriched in ^{18}O and ^{2}H than the flat area when assessing the sites as a whole. Looking closer, the samples collected at 10 cm and 20 cm in the channelized area have a large range that encompasses the $\delta^{18}O$ range of the 10 cm and 20 cm samples in the flat area. The $\delta^{2}H$ range of the samples collected at 20 cm in the channelized area shows this same trend. However,

the δ^2H range of the samples collected at 10 cm in the channelized area is more depleted in ^2H than that of the 10 cm samples from the flat area.

Table 1: Range of values for $\delta^{18}O$ and δ^2H (‰) in precipitation, vegetation, and soil samples.

	$\delta^{18}O$			δ^2H		
	Minimum	**Maximum**	**Mean**	**Minimum**	**Maximum**	**Mean**
Precipitation	-16.88 ‰	11.00 ‰	**-4.80 ‰**	-134.17 ‰	37.36 ‰	**-38.84 ‰**
All Mesquite	-6.09 ‰	9.99 ‰	**-0.94 ‰**	-70.19 ‰	4.69 ‰	**-48.39 ‰**
CA Mesquite	-4.34 ‰	9.99 ‰	**0.12 ‰**	-57.26 ‰	4.69 ‰	**-40.28 ‰**
FA Mesquite	-6.09 ‰	2.48 ‰	**-2.00 ‰**	-70.19 ‰	-40.17 ‰	**-56.50 ‰**
All Creosote	-7.62 ‰	17.91 ‰	**1.74 ‰**	-85.36 ‰	13.50 ‰	**-41.85 ‰**
CA Creosote	-7.62 ‰	11.05 ‰	**-1.11 ‰**	-85.36 ‰	-20.39 ‰	**-52.63 ‰**
FA Creosote	-1.53 ‰	17.91 ‰	**4.59 ‰**	-61.65 ‰	13.50 ‰	**-31.07 ‰**
All Soil 10cm	-17.32 ‰	4.77 ‰	**-5.32 ‰**	-89.49 ‰	-9.87 ‰	**-49.67 ‰**
CA Soil 10cm	-17.32 ‰	4.77 ‰	**-6.22 ‰**	-89.49 ‰	-9.87 ‰	**-52.28 ‰**
FA Soil 10cm	-12.76 ‰	4.73 ‰	**-4.43 ‰**	-79.71 ‰	-8.70 ‰	**-47.06 ‰**
All Soil 20cm	-16.97 ‰	5.28 ‰	**-6.76 ‰**	-96.89 ‰	-7.90 ‰	**-51.18 ‰**
CA Soil 20cm	-16.97 ‰	5.28 ‰	**-7.37 ‰**	-96.89 ‰	-7.90 ‰	**-53.58 ‰**
FA Soil 20cm	-13.76 ‰	2.65 ‰	**-6.14 ‰**	-75.55 ‰	-13.81 ‰	**-48.79 ‰**
All CA Soil	-17.32 ‰	5.28 ‰	**-6.79 ‰**	-96.89 ‰	-7.90 ‰	**-52.93 ‰**
All FA Soil	-13.76 ‰	4.73 ‰	**-5.29 ‰**	-79.71 ‰	-8.70 ‰	**-47.93 ‰**

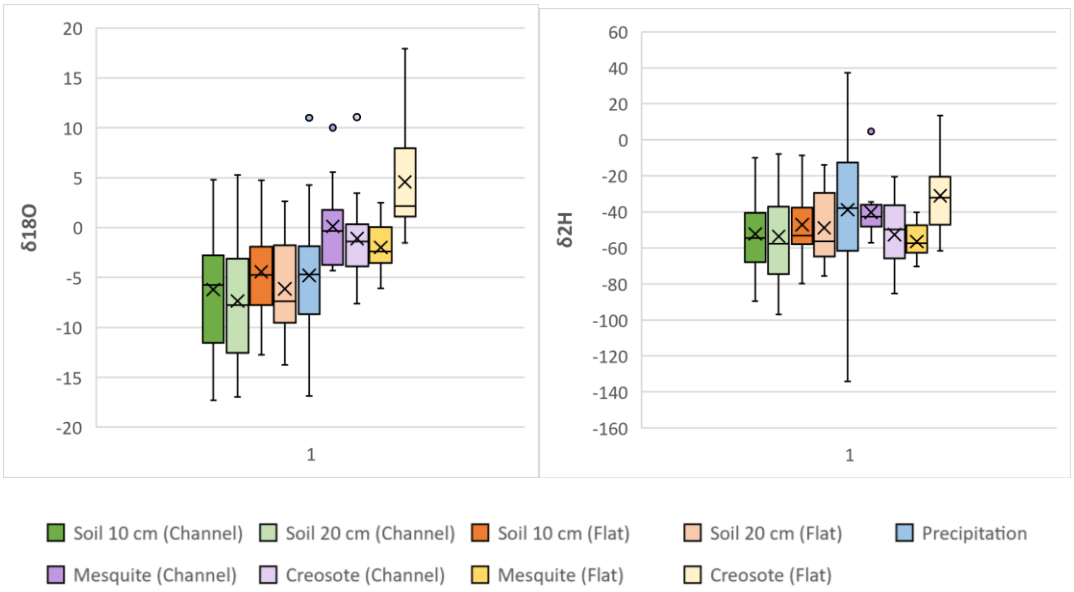

Figure 16: Box and whisker plots of $\delta^{18}O$ and $\delta^{2}H$ in soil, precipitation, and vegetation samples. The mean value for each is marked with an 'x' and outlier values are plotted in circles.

The $\delta^{18}O$ of precipitation shows a general trend of enrichment in ^{18}O as the year progressed from October 2018 to August 2019 (Figure 17). The values then steadily become more depleted in ^{18}O as the year progressed into fall and winter. The $\delta^{18}O$ of the soils collected from both study sites have a similar trend; however, soils from the flat area (Site 2) seem to follow the trend of precipitation a little closer than the soils collected in the channelized area (Site 1). At the beginning of the study period, the $\delta^{18}O$ of the channel area soils and the flat area soils varied and plotted apart from each other. As the year progressed into summer, their $\delta^{18}O$ values became more similar and plotted closer together. This trend appears to be tied to the seasonality of rainfall in the study area: there are small, spaced-out precipitation events that occur during the winter (beginning of the study period), then as the season progresses into the summer there are larger events that occur much closer together. Some of the larger precipitation events during this period raised soil moisture content to saturation at 10 and 20 cm depths, as seen in the soil moisture series measured by the SEL (Figure 17).

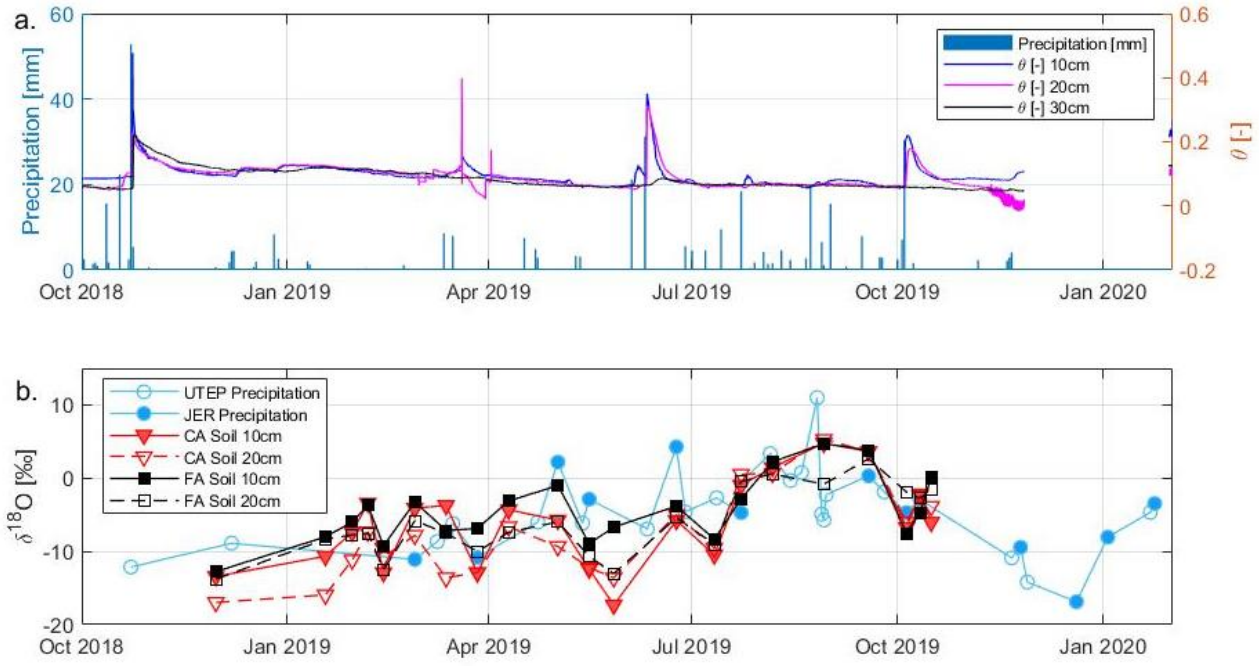

Figure 17: Time series plots of precipitation and soil moisture collected during the study period. (a) Daily precipitation plotted with soil moisture (θ) at three depths (10 cm, 20 cm, and 30 cm). (b) $\delta^{18}O$ (‰) of precipitation is compared to $\delta^{18}O$ (‰) of channel area (CA) and flat area (FA) soils (at 10 cm and 20 cm).

3.3.2 Precipitation and Vegetation Stem Water

The $\delta^{18}O$ and $\delta^{2}H$ ranges of vegetation stem water coincide with that of precipitation during the study period (Figure 16 and Table 1). The average $\delta^{18}O$ of mesquite and creosote samples are more enriched in ^{18}O than the precipitation samples, while the average $\delta^{2}H$ of precipitation is slightly more enriched in ^{2}H than the vegetation samples. This overlap in $\delta^{18}O$ and $\delta^{2}H$ signatures is evident in Figure 18. The precipitation samples show a significant seasonality, more enriched in ^{18}O in the warm spring and summer months and depleted in ^{18}O in the cooler fall and winter months. The $\delta^{18}O$ of mesquite and creosote collected from both study areas have a similar trend during the warmer months (~May to September). The samples plot close to each other during this time period. However, in early October 2019, the vegetation samples began to have signatures that are more enriched in ^{18}O than that of precipitation. Not only do the four vegetation samples plot differently than the precipitation during this second half of the study period, but they also plot separately from each other. Then, at the very end of the study period, the vegetation signatures start to plot close to the precipitation signatures again.

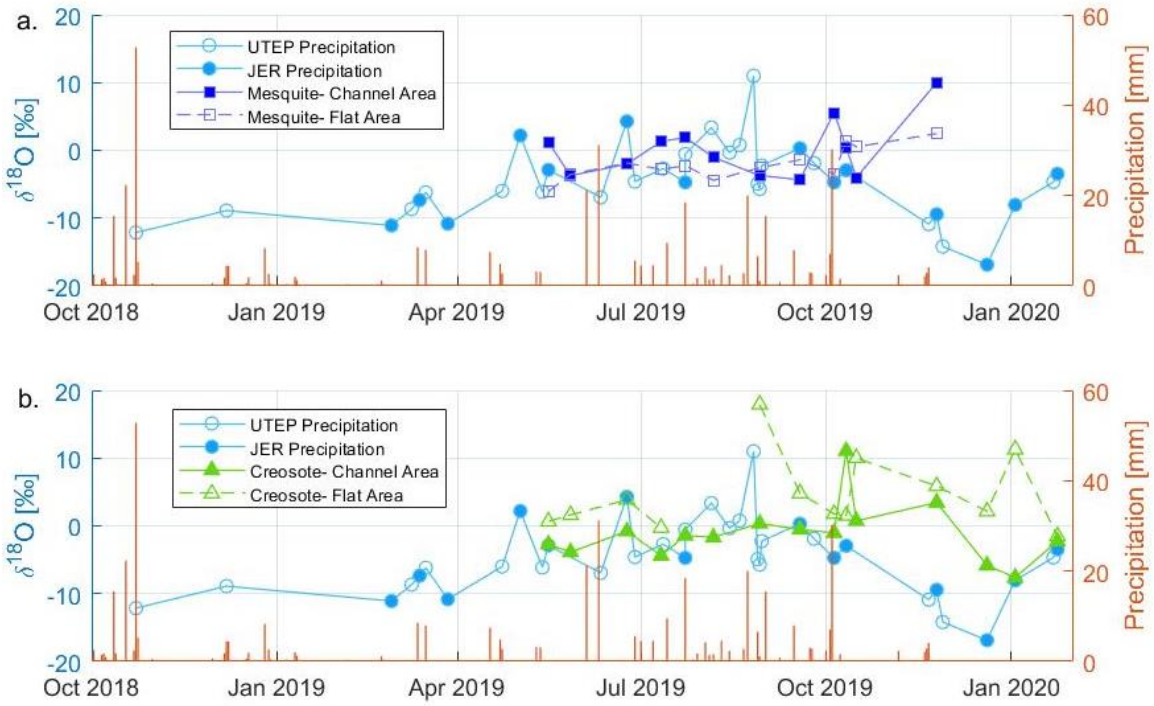

Figure 18: Time series plot of precipitation and vegetation collected during the study period. (a) Daily precipitation (mm) plotted with $\delta^{18}O$ (‰) of precipitation and mesquite samples. (b) Daily precipitation (mm) plotted with $\delta^{18}O$ (‰) of precipitation and creosote samples. Light blue circles represent the $\delta^{18}O$ of precipitation samples collected from the two rain collectors. Dark blue squares represent the $\delta^{18}O$ of mesquite samples collected from the two study areas. Green triangles represent the $\delta^{18}O$ of creosote samples collected from the two study areas.

3.3.3 Soil Water and Vegetation Stem Water

The $\delta^{18}O$ and $\delta^{2}H$ isotopic signatures of vegetation stem water samples and soil water samples also overlap during the study period (Figure 16 and Table 1). However, the $\delta^{18}O$ and $\delta^{2}H$ signatures of soil water samples are more depleted in ^{18}O and ^{2}H than that of the vegetation samples during the majority of the year (Figures 19 and 20). In the channel area, soil water samples and both the mesquite and creosote samples only coincide from July to October 2019. In the flat area, the creosote samples show a similar trend of overlapping with soil water samples only between July to October 2019. Meanwhile, the mesquite samples in the flat area appear to correspond with the soil water samples for most of the samplings from May to October 2019.

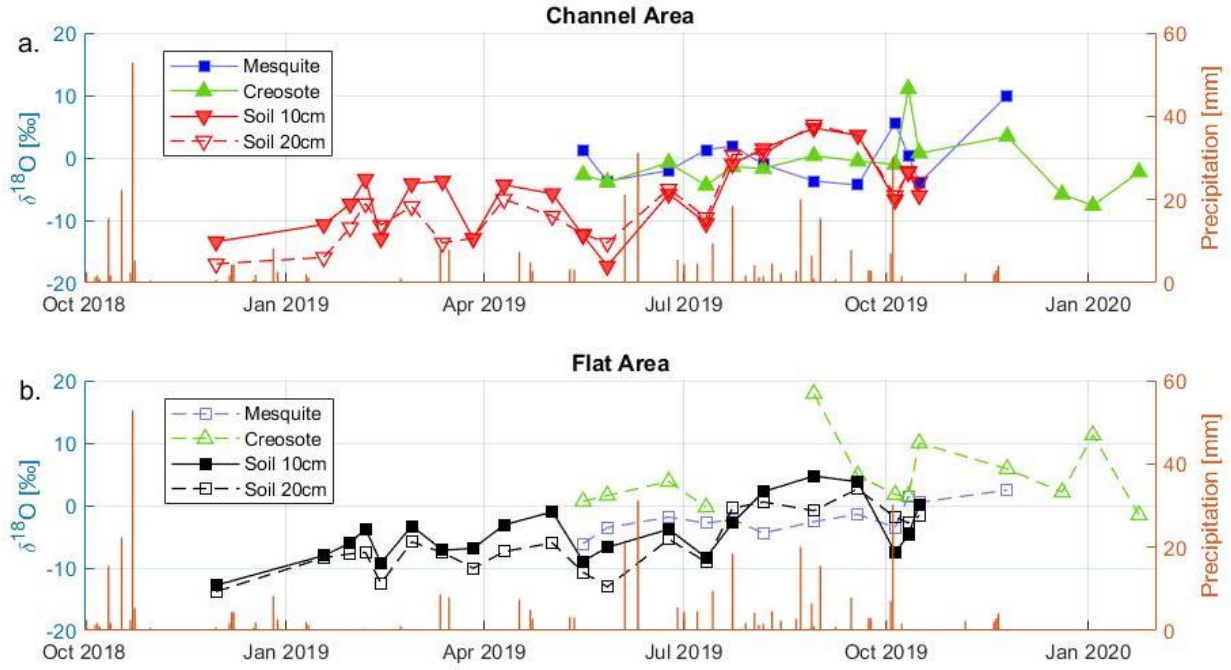

Figure 19: Time series plots of vegetation and soil collected during the study period. (a) $\delta^{18}O$ (‰) values of vegetation and soil collected in the channel area (Site 1). (b) $\delta^{18}O$ (‰) values of vegetation and soil collected in the flat area (Site 2).

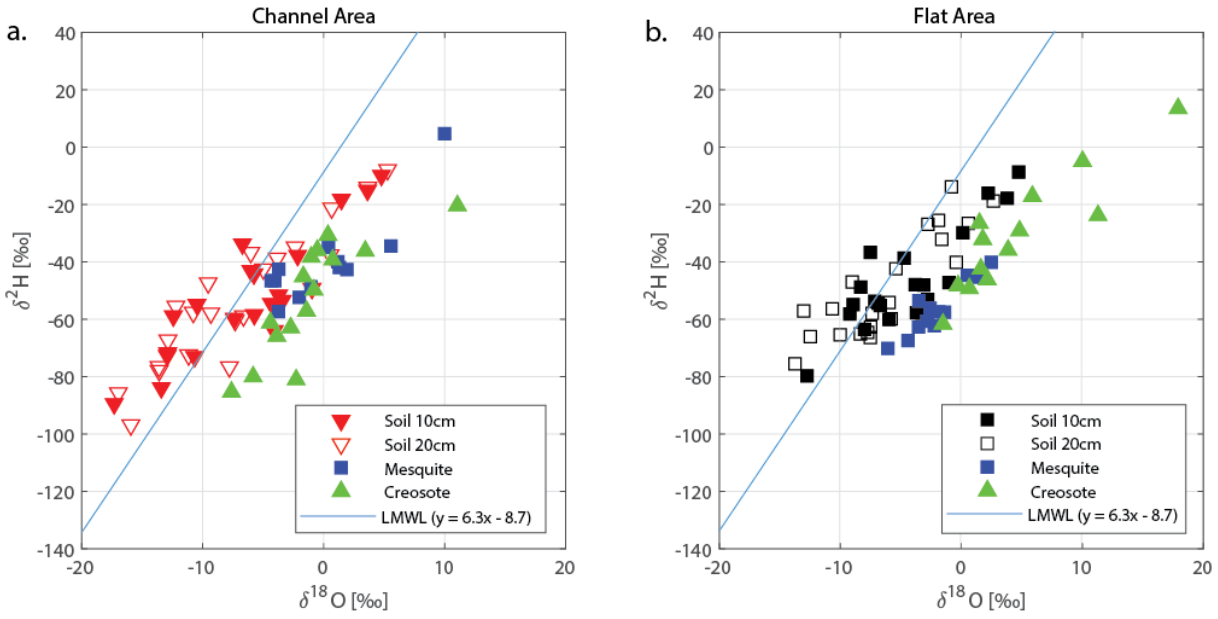

Figure 20: Plots of $\delta^{18}O$ vs $\delta^{2}H$ (‰) for vegetation and soil during the study period. (a) Soil samples plotted with mesquite and creosote samples collected from the channel area (Site 1). (b) Soil samples plotted with mesquite and creosote samples collected from the flat area (Site 2).

Chapter 4: Discussion

4.1 Location Influence on Isotopic Composition

We hypothesized that the location of the plants and their associated soil within the landscape would have an effect on their isotopic signature because they could contain distinct characteristics or undergo different processes. We sampled from two study sites in the JER to test this hypothesis: a low-lying channelized area (Site 1) and a slightly elevated flat area (Site 2). Our results indicate that the position in the landscape has an effect on the isotopic composition of soil water, and thus influences the type of water the plants use.

When assessing the soil water isotopic signatures, it is clear that although the samples from both study sites have overlapping ranges of values, they have distinctly different behaviors. Our results found that the isotopic composition of the soil water in the channel area becomes more enriched in ^{18}O and ^{2}H (or more depleted) faster than the soil water in the flat area (Figure 12). This 'behavior' causes the soil samples from the channel area to have a larger range of values than that of the flat area (Figures 11, 16, and 20). A possible explanation for this behavior is that the channel area is receiving water runoff from upstream that has a distinct isotopic signature that combines with water previously in the soil profile. Since the flat area is located slightly higher in elevation and does not contain as many small arroyos as the channel area, the soil may be receiving water mostly from local precipitation, while the channel area soil could be receiving a greater mix of local and upstream precipitation. This could explain why the isotopic signatures of our flat area soil water samples have a more similar trend to that of our precipitation samples than the channel area (Figure 17). Also, if the runoff from upstream was derived from a precipitation event that resulted in rainfall that was extremely depleted in ^{18}O and ^{2}H it could also explain why the flat area and, to a greater extent, the channel area contains soil water samples with very low $\delta^{18}O$ and $\delta^{2}H$ signatures (Figure 11). Rainfall that is extremely depleted in ^{18}O and ^{2}H can be achieved

through various processes, such as precipitation events that occur at higher elevations with lower average temperatures (Clark and Fritz, 1997), or large, intense precipitation events that cause increased rainout effects from Rayleigh distillation of heavy isotopes (Clark and Fritz, 1997; Dansgaard, 1964; Brooks et al., 2010).

Similar to our soil water samples, the vegetation stem water samples exhibit distinct behaviors in the two study sites. In the channel area, creosote samples are generally more depleted in ^{18}O and ^{2}H than mesquite samples (Figures 16 and 20). Whereas, in the flat area, the behavior is reversed: the mesquite samples are generally more depleted in ^{18}O and ^{2}H than the creosote. Although our vegetation stem water samples were more enriched in ^{18}O and ^{2}H relative to the soil water samples, there are patterns in their isotopic compositions that lend to possible source interpretation. We observe that the isotopic composition of the creosote stem water samples follows the trend of the average $\delta^{18}O$ and $\delta^{2}H$ values of soil water for a given site. For instance, the channel area soil water was on average more depleted in ^{18}O and ^{2}H than that of the flat area, and the creosote stem water samples were also more depleted in comparison to the mesquite samples. Similarly, the soil water in the flat area was on average more enriched in ^{18}O and ^{2}H, and the creosote stem water was also enriched at that site. This finding is a possible indication of the dexterity of the creosote shrub to find viable water sources year-round. Creosotes are well adapted to arid and semiarid landscapes due to their ability to use extremely shallow soil water and shift their patterns of activity to take advantage of obtainable water resources (Reynolds et al., 1999; Peters and Gibbens, 2006). This is supported by the large range of $\delta^{18}O$ and $\delta^{2}H$ for creosote stem water in both study sites: they attempt to use any source of water available to them. Mesquite stem water samples behave somewhat adversely, especially in the flat area (Figure 20). They exhibit a smaller range of $\delta^{18}O$ and $\delta^{2}H$, indicating a possible preference for a specific source.

4.2 Variability of Isotopic Composition in Precipitation and Soil Water

The $\delta^{18}O$ and $\delta^{2}H$ isotopic composition of our precipitation samples had a seasonal pattern of variation over the 15-month study period (October 2018 – January 2020). Consistent with previous studies, the summer monsoonal precipitation was enriched in ^{18}O and ^{2}H, while precipitation during the winter dry season was depleted in ^{18}O and ^{2}H (Figure 9) (Dansgaard, 1964; Clark and Fritz, 1997; Wright et al., 2001; Hu and Dominguez, 2015; Eastoe and Dettman, 2016). During the monsoon season (June – October), precipitation samples had an average $\delta^{18}O$ value of -1.92 ‰ and an average $\delta^{2}H$ value of -16.34 ‰. Whereas, in the dry season (November – May), the samples had an average $\delta^{18}O$ value of -7.84 ‰ and an average $\delta^{2}H$ value of -62.67 ‰. Research by Wright et al. (2001) and Hu and Dominguez (2015) found that precipitation events from the Gulf of Mexico and the Caribbean Sea are more isotopically enriched in ^{18}O and ^{2}H than those events from the Gulf of California and the Pacific Ocean. Our research supports these findings: the majority of summer monsoonal precipitation in the JER is derived from the Gulf of Mexico and winter precipitation is derived from the Pacific Ocean (Ji et al., 2019; Peters and Eve, 1995; Wainwright 2006). The seasonal variability of the precipitation samples is also recorded by the LMWL ($\delta^{2}H = 6.3*\delta^{18}O - 8.7‰$) that was derived from our samples (Figure 10). According to Clark and Fritz (1997), a slope less than 8 indicates that summer precipitation was primarily derived from tropical/equatorial sources, and it has been subjected to evaporation during the rainfall event.

Predictably, the soil water contains isotopic signatures with similar seasonal trends to that of precipitation in the JER (Figure 17). This further substantiates their connection in soil-vegetation-atmosphere dynamics. Consistent with previous research, our results support that isotopic composition of the soil water becomes progressively enriched in ^{18}O and ^{2}H at shallow depths due to increased fractionation from evaporation (Clark and Fritz, 1997; Barnes and Allison,

1988; Szutu and Papuga, 2019). On average, the soil water samples taken at 10 cm were slightly more enriched in ^{18}O and ^{2}H than those at 20 cm, in both study sites (Figure 16 and Table 1). Our results also found that the soil samples taken at a depth of 10 cm behave differently that the samples taken at a depth of 20 cm. The soil samples taken at 10 cm become more enriched (or depleted) in ^{18}O faster than the 20 cm samples (Figure 13). This finding was foreseeable, as it indicates that the soil nearest to the surface is more affected by changing atmospheric and environmental conditions than the soil deeper in the profile.

4.3 Indications of Tightly Bound Soil Water

Our research exhibits indications of the existence of tightly bound soil water and its possible use by mesquite and creosote within the Jornada Experimental Range (JER). Looking at the $\delta^{18}O$ and $\delta^{2}H$ of soil water from both study sites, approximately one-third of the data falls to the left of the LMWL (Figure 11). This is normally an indication of deuterium excess or ^{18}O depletion caused by secondary evaporation of precipitation from local surface waters in low-humidity regions (Clark and Fritz, 1997). However, this characteristic is not found in the precipitation samples that we collected from October 2018 – January 2020 (Figure 10); it is only exhibited in our soil water samples from November 2018 – June 2019 (Figures 17 and 19). We realize that the occurrence of these values that are highly depleted in ^{18}O and ^{2}H is rare (Clark and Fritz, 1997), and that it could be evidence of human or machine errors during the sampling or analysis. However, it is also possible that the values could be indicative of a rainfall event that underwent secondary evaporation just prior to our study period and was tightly bound within the soils of our study area until June 2019.

Since values that are extremely depleted in ^{18}O and ^{2}H only occur in our soil water samples at the beginning of our study (~November 2018 – June 2019), they only coincide with two of our

vegetation sample dates (Figure 19). There is a possibility that the plants were taking up this tightly bound water during the beginning of our study period, but it is not seen in our first two vegetation samples that overlap in time with the exceptionally depleted soil water. However, immediately following this time period, there were two large precipitation events that occurred in the JER on June 4, 2019 and June 10, 2019. The very next sampling date (June 24, 2019) exhibits $\delta^{18}O$ and $\delta^{2}H$ of soil water and vegetation stem water samples from both study sites plotted very closely together (Figure 19). The isotopic composition of our vegetation samples following this date remain relatively steady until another large precipitation event in October 2019, despite changes in precipitation and soil water $\delta^{18}O$ and $\delta^{2}H$ values during this time. We propose that these two rainfalls in early June 2019 could act as the first major precipitation event after the dry season and may support recent ecohydrological research that suggests that tightly bound soil water is stored from this event (Brooks et al., 2010; Goldsmith et al., 2011; McDonnell 2014; Penna et al., 2013). However, instead of this tightly bound soil water remaining in the soil until the next dry season (November 2019 – May 2020) for use by vegetation, it was taken up by vegetation in-between summer precipitation events when temperatures and ET were at their highest. It is possible that the next large precipitation event on October 4, 2019, was also tightly bound and stored in the soil for vegetation use for the dry season—as indicated by the $\delta^{18}O$ and $\delta^{2}H$ of soil water and vegetation stem water samples from both study sites plotting closely together again (Figure 19).

Chapter 5: Conclusions

Results from our 15-month study in the Jornada Experimental Range (JER) of the Northern Chihuahuan Desert show that there are distinct patterns and processes associated with the water available for use by the honey mesquite and creosote shrubs throughout the year. We found that the location of the vegetation and their associated soil in the landscape has an effect on the isotopic composition of the water they use. Our results revealed that the soil water from the channel and flat areas had distinctly different behaviors: the channel area soil water became more enriched (or depleted) in ^{18}O and ^{2}H faster than the flat area. We suggest that this behavior could be the result of the channel area receiving isotopically distinct water runoff from upstream that combines with local precipitation already present in the soil. This is supported by the flat area soil water samples following the trend of our precipitation samples more closely than the channel area. Similarly, our vegetation stem water samples exhibited different behaviors in the two study sites. In the channel area, creosote samples were more depleted in ^{18}O and ^{2}H in comparison to the mesquite, whereas, in the flat area, mesquite samples were more depleted in ^{18}O and ^{2}H than the creosotes. Our results revealed that the creosote stem water samples followed the average $\delta^{18}O$ and $\delta^{2}H$ behavior of the soil water at the site they were located in. The soil water in the channel area was more depleted in ^{18}O and ^{2}H, on average, and so was the creosotes in comparison to the mesquites. In the flat area, the soil water was on average more enriched in ^{18}O and ^{2}H, as well as the creosotes. We argue that this is an indication of their resilience and efficiency in arid and semi-arid environments to change their behavior to take advantage of available resources. This was supported by their large range of $\delta^{18}O$ and $\delta^{2}H$ in both sites.

Our results also revealed that precipitation and soil water samples from the JER have a seasonal variation in their isotopic compositions. In the warm summer months (June – October),

when monsoonal rainfall is derived from the Gulf of Mexico, our precipitation and soil water samples are isotopically enriched in ^{18}O and ^{2}H. In the winter dry season (November – May), when small, sporadic rainfall events are derived from the Pacific Ocean, our precipitation and soil water samples are isotopically depleted in ^{18}O and ^{2}H. Our results also found that the soil water samples varied spatially by depth. Similar to previous studies, the soil water samples collected at 10 cm were slightly more enriched in ^{18}O and ^{2}H than those collected at a depth of 20 cm, at both of the study sites (Clark and Fritz, 1997; Barnes and Allison, 1988; Szutu and Papuga, 2019).

In this work, we also found indications of tightly bound soil water in the JER. A group of the soil water samples from the beginning of our study fall on the left side of the LMWL, implying that the water source underwent secondary evaporation to cause deuterium excess. However, during the course of our study, we did not detect this characteristic in our precipitation or vegetation samples. We suggest that a precipitation event with this distinct trait could have occurred prior to our study, and the water was tightly bound in the soil until the next large precipitation event. This is supported by patterns in our vegetation stem samples. Following two large precipitation events in June 2019, vegetation and soil water samples exhibit similar $\delta^{18}O$ and $\delta^{2}H$. The vegetation stem water samples have relatively consistent isotopic signatures until the next large precipitation event in October 2019, despite changes in precipitation and soil water values. We argue that the large precipitation events in June supplied water to the soil and became tightly bound. During this time (June – October 2019) when temperature and evaporative demand was high, the vegetation accessed the tightly bound soil water to remain active. After the large precipitation event in October 2019, vegetation and soil water samples exhibit similar $\delta^{18}O$ and $\delta^{2}H$ again. This could be indicative of the soil receiving more water to be tightly bound and accessible to the vegetation over the winter dry season.

Similar to other studies, our results indicate that stable isotopes of $\delta^{18}O$ and $\delta^{2}H$ associated with vegetation stem water can be complex to analyze and interpret (Brooks et al., 2010; McDonnell, 2014; Johnson et al., 2017; Szutu et al., 2019). Our vegetation stem samples had to be salvaged and reanalyzed for $\delta^{18}O$ and $\delta^{2}H$ due to the presence of volatile organic compounds distorting our original results. Once reanalyzed, our $\delta^{18}O$ and $\delta^{2}H$ for vegetation were difficult to interpret. The vegetation stem water samples were generally more enriched in ^{18}O and ^{2}H than the soil water and precipitation samples. This could indicate that we did not consider all possible sources of water for the plants or did not account for fractionation processes occurring in our samples. Despite problems with our original analysis and difficulties interpreting the data from the vegetation stem water isotopes, we were still able to identify possible indications from our results and make suggestions for continued research in arid and semi-arid environments.

5.1 Future Work

Future work should incorporate a longer dataset with continuous biweekly sampling of soils, vegetation and rainfall, taking into consideration other possible water sources for the vegetation, such as deeper soil moisture and water held in the caliche horizons. It should also consider processes that could be affecting soil water. For example, samples of precipitation and soil could be gathered at upstream locations to assess their influence, if any, on the water in the channel area soil samples. Soil samples should also be gathered from shallower and deeper depths, if possible, to determine whether water held in those horizons are used by the vegetation. This research could benefit from a full isotopic soil profile. An additional topic of interest to complement this study would be to continue taking precipitation, soil water, and stem water samples in the JER to determine the cause of findings of deuterium excess in the soil water samples and better understand the effects of hydrologic recycling within arid and semi-arid environments.

References

Ansley, R.J., Jacoby, P.W., and Cuomo, G.J., 1990, Water Relations of Honey Mesquite following Severing of Lateral Roots: Influence of Location and Amount of Subsurface Water: Journal of Range Management, v. 43, p. 436–441, doi: 10.2307/3899008.

Barnes, C., and Allison, G., 1988, Tracing of water movement in the unsaturated zone using stable isotopes of hydrogen and oxygen: Journal of Hydrology, v. 100, p. 143–176, doi: 10.1016/0022-1694(88)90184-9.

Brooks, J.R., Barnard, H.R., Coulombe, R., and McDonnell, J.J., 2010, Ecohydrologic separation of water between trees and streams in a Mediterranean climate: Nature Geoscience, v. 3, p. 100–104, doi: 10.1038/ngeo722.

Clark, I.D., and Fritz, P., 1997, Environmental Isotopes in Hydrogeology: CRC Press.

Craig, H., 1961, Isotopic Variations in Meteoric Waters: Science, v. 133, p. 1702–1703, doi: 10.1126/science.133.3465.1702.

Dansgaard, W., 1964, Stable isotopes in precipitation: Tellus, v. 16, p. 436–468, doi: 10.3402/tellusa.v16i4.8993.

Darrouzet-Nardi, A., D'Antonio, C.M., and Dawson, T.E., 2006, Depth of water acquisition by invading shrubs and resident herbs in a Sierra Nevada meadow: Plant and Soil, v. 285, p. 31–43, doi: 10.1007/s11104-005-4453-z.

Dawson, T.E., and Ehleringer, J.R., 1991, Streamside trees that do not use stream water: Nature, v. 350, p. 335–337, doi: 10.1038/350335a0.

Document Library: A0211 and A0325 (High Precision Vaporizer and Auto Sampler) Datasheet, 2014, PICARRO INC., https://www.picarro.com/support/library/documents/a0211_and_a0325_high_precision_vaporizer_and_auto_sampler_datasheet_data (accessed May 2019).

Document Library: A0213 (Induction Module) Datasheet, 2013, PICARRO INC., https://www.picarro.com/support/library/documents/a0213_induction_module_datasheet_data_sheet (accessed May 2019).

Duniway, M.C., Herrick, J.E., and Monger, H.C., 2007, The High Water-Holding Capacity of Petrocalcic Horizons: Soil Science Society of America Journal, v. 71, p. 812–819, doi: 10.2136/sssaj2006.0267.

Duniway, M.C., Herrick, J.E., and Monger, H.C., 2009, Spatial and temporal variability of plant-available water in calcium carbonate-cemented soils and consequences for arid ecosystem resilience: Oecologia, v. 163, p. 215–226, doi: 10.1007/s00442-009-1530-7.

Durner, W., Iden, S.C., Schelle, H., and Peters, A., 2011, Determination of hydraulic properties of porous media across the whole moisture range: Proceedings CMM Conference , p. 1–13.

Eastoe, C., and Dettman, D., 2016, Isotope amount effects in hydrologic and climate reconstructions of monsoon climates: Implications of some long-term data sets for precipitation: Chemical Geology, v. 430, p. 78–89, doi: 10.1016/j.chemgeo.2016.03.022.

Gibbens, R., Mcneely, R., Havstad, K., Beck, R., and Nolen, B., 2005, Vegetation changes in the Jornada Basin from 1858 to 1998: Journal of Arid Environments, v. 61, p. 651–668, doi: 10.1016/j.jaridenv.2004.10.001.

Gile, L., Gibbens, R., and Lenz, J., 1998, Soil-induced variability in root systems of creosotebush (Larrea tridentata) and tarbush (Flourensia cernua): Journal of Arid Environments, v. 39, p. 57–78, doi: 10.1006/jare.1998.0377.

Goldsmith, G.R., Muñoz-Villers, L.E., Holwerda, F., Mcdonnell, J.J., Asbjornsen, H., and Dawson, T.E., 2011, Stable isotopes reveal linkages among ecohydrological processes in a seasonally dry tropical montane cloud forest: Ecohydrology, v. 5, p. 779–790, doi: 10.1002/eco.268.

Gutiérrez-Jurado, H.A., Vivoni, E.R., Harrison, J.B.J. and Guan, H. 2006. Ecohydrology of root-zone water fluxes and soil development in complex semiarid rangelands. *Hydrological Processes*. 20(15): 3289-3316.

Gubiani, P.I., Reichert, J.M., Campbell, C., Reinert, D.J., and Gelain, N.S., 2013, Assessing Errors and Accuracy in Dew-Point Potentiometer and Pressure Plate Extractor Measurements: Soil Science Society of America Journal, v. 77, p. 19–24, doi: 10.2136/sssaj2012.0024.

Havstad, K.M., Huenneke, L.F., and Schlesinger, W.H. (Eds.), 2006, Structure and Function of a Chihuahuan Desert Ecosystem: The Jornada Basin Long-Term Ecological Research Site: New York, NY, Oxford University Press.

Hu, H., and Dominguez, F., 2015, Evaluation of Oceanic and Terrestrial Sources of Moisture for the North American Monsoon Using Numerical Models and Precipitation Stable Isotopes: Journal of Hydrometeorology, v. 16, p. 19–35, doi: 10.1175/jhm-d-14-0073.1.

Ji, W., Hanan, N.P., Browning, D.M., Monger, H.C., Peters, D.P.C., Bestelmeyer, B.T., Archer, S.R., Ross, C.W., Lind, B.M., Anchang, J., Kumar, S.S., and Prihodko, L., 2019, Constraints on shrub cover and shrub-shrub competition in a U.S. southwest desert: Ecosphere, v. 10, p. 1–16, doi: 10.1002/ecs2.2590.

Johnson, J.E., Hamann, L., Dettman, D.L., Kim-Hak, D., Leavitt, S.W., Monson, R.K., and Papuga, S.A., 2017, Performance of induction module cavity ring-down spectroscopy (IM-CRDS) for measuring δ18O and δ2H values of soil, stem, and leaf waters: Rapid Communications in Mass Spectrometry, v. 31, p. 547–560, doi: 10.1002/rcm.7813.

Li, S.-G., Romero-Saltos, H., Tsujimura, M., Sugimoto, A., Sasaki, L., Davaa, G., and Oyunbaatar, D., 2007, Plant water sources in the cold semiarid ecosystem of the upper Kherlen River catchment in Mongolia: A stable isotope approach: Journal of Hydrology, v. 333, p. 109–117, doi: 10.1016/j.jhydrol.2006.07.020.

McDonnell, J.J., 2014, The two water worlds hypothesis: ecohydrological separation of water between streams and trees?: Wiley Interdisciplinary Reviews: Water, v. 1, p. 323–329, doi: 10.1002/wat2.1027.

Monger, H.C., 2006, Soil Development in the Jornada Basin, in Havstad, K.M., Huenneke, L.F., and Schlesinger, W.H., eds., Structure and Function of a Chihuahuan Desert Ecosystem: The Jornada Basin Long-Term Ecological Research Site: New York, NY, Oxford University Press, p. 81-106.

Monger, H.C., Mack, G.H., Nolen, B.A., Gile, L.H., 2006, Regional Setting of the Jornada Basin, in Havstad, K.M., Huenneke, L.F., and Schlesinger, W.H., eds., Structure and Function of a Chihuahuan Desert Ecosystem: The Jornada Basin Long-Term Ecological Research Site: New York, NY, Oxford University Press, p. 15-43.

Nobles, M., Wilding, L., and Lin, H., 2010, Flow pathways of bromide and Brilliant Blue FCF tracers in caliche soils: Journal of Hydrology, v. 393, p. 114–122, doi: 10.1016/j.jhydrol.2010.03.014.

Orlowski, N., Frede, H.-G., Brüggemann, N., and Breuer, L., 2013, Validation and application of a cryogenic vacuum extraction system for soil and plant water extraction for isotope analysis: Journal of Sensors and Sensor Systems, v. 2, p. 179–193, doi: 10.5194/jsss-2-179-2013.

Penna, D., Oliviero, O., Assendelft, R., Zuecco, G., Meerveld, I.(H.J.V., Anfodillo, T., Carraro, V., Borga, M., and Fontana, G.D., 2013, Tracing the Water Sources of Trees and Streams: Isotopic Analysis in a Small Pre-Alpine Catchment: Procedia Environmental Sciences, v. 19, p. 106–112, doi: 10.1016/j.proenv.2013.06.012.

Peters, A.J., and Eve, M.D., 1995, Satellite Monitoring of Desert Plant Community Response to Moisture Availability: Environmental Monitoring and Assessment, v. 37, p. 273–287, doi: 10.1007/978-94-009-1635-7_20.

Peters, D.P.C., and Gibbens, R.P., 2006, Plant Communities in the Jornada Basin: The Dynamic Landscape, in Havstad, K.M., Huenneke, L.F., and Schlesinger, W.H., eds., Structure and Function of a Chihuahuan Desert Ecosystem: The Jornada Basin Long-Term Ecological Research Site: New York, NY, Oxford University Press, p. 15-43.

Querejeta, J.I., Estrada-Medina, H., Allen, M.F., and Jiménez-Osornio, J.J., 2007, Water source partitioning among trees growing on shallow karst soils in a seasonally dry tropical climate: Oecologia, v. 152, p. 26–36, doi: 10.1007/s00442-006-0629-3.

Reynolds, J.F., Kemp, P.R., and Tenhunen, J.D., 2000, Effects of long-term rainfall variability on evapotranspiration and soil water distribution in the Chihuahuan Desert: A modeling analysis: Plant Ecology, v. 150, p. 145–159.

Reynolds, J.F., Virginia, R.A., Kemp, P.R., Soyza, A.G.D., and Tremmel, D.C., 1999, Impact Of Drought On Desert Shrubs: Effects Of Seasonality And Degree Of Resource Island Development: Ecological Monographs, v. 69, p. 69–106, doi: 10.1890/0012-9615(1999)069[0069:iodods]2.0.co;2.

Schindler, U., Unold, G.V., Durner, W., and Mueller, L., 2015, Recent Progress in Measuring Soil Hydraulic Properties: International Academy of Engineers (IA-E), p. 47–52, doi: 10.15242/iae.iae0415401.

Schmidt, R.H., 1979, A climatic delineation of the ‘real’ Chihuahuan Desert: Journal of Arid Environments, v. 2, p. 243–250, doi: 10.1016/s0140-1963(18)31774-9.

Solone, R., Bittelli, M., Tomei, F., and Morari, F., 2012, Errors in water retention curves determined with pressure plates: Effects on the soil water balance: Journal of Hydrology, v. 470-471, p. 65–74, doi: 10.1016/j.jhydrol.2012.08.017.

Szutu, D.J., and Papuga, S.A., 2019, Year-Round Transpiration Dynamics Linked With Deep Soil Moisture in a Warm Desert Shrubland: Water Resources Research, v. 55, p. 5679–5695, doi: 10.1029/2018wr023990.

Wainwright, J., 2006, Climate and Climatological Variations in the Jornada Basin, in Havstad, K.M., Huenneke, L.F., and Schlesinger, W.H., eds., Structure and Function of a Chihuahuan Desert Ecosystem: The Jornada Basin Long-Term Ecological Research Site: New York, NY, Oxford University Press, p. 44-80.

Wright, W.E., Long, A., Comrie, A.C., Leavitt, S.W., Cavazos, T., and Eastoe, C., 2001, Monsoonal moisture sources revealed using temperature, precipitation, and precipitation stable isotope timeseries: Geophysical Research Letters, v. 28, p. 787–790, doi: 10.1029/2000gl012094.

APPENDIX A: PROTOCOL FOR COLLECTING PRECIPITATION, STEM, AND SOIL SAMPLES FOR ISOTOPIC ANALYSIS WITH THE PICARRO L2130-I ANALYZER

Hayden E. Thompson[1]

[1]Department of Geological Sciences, University of Texas at El Paso, El Paso, TX 79968, USA

1. SUMMARY

This appendix describes the protocol that was used for collecting precipitation, stem, and soil samples at the study area. The study area consists of two locations on the piedmont slope of the Jornada Experimental Range of the Northern Chihuahuan Desert. Samples are collected at a two-week interval from two sites: the channelized area (Site 1) and the flat area (Site 2). Precipitation samples are collected in a plastic tube using a rainfall collector with a few centimeters of mineral oil to prevent evaporation. Stem samples are collected from two Mesquites and two Creosotes from each site. Soil samples are collected in glass jars at 10-centimeter and 20-centimeter depths from each site, taken in locations between the plants of interest in that area. All samples are wrapped in laboratory film (e.g. parafilm) and placed into a cooler with ice packs during transportation to the lab. In the lab, all samples are placed into the refrigerator until they can be analyzed.

2. SITE DESCRIPTION

The study area is located on the piedmont slope of the Jornada Experimental Range (JER) of the Northern Chihuahuan Desert. The JER is situated in south-central New Mexico, 30 km northeast of Las Cruces, within the Jornada Basin Long-Term Ecological Research (LTER) site. The Jornada Basin LTER is bordered by the Rio Grande Valley to the west and the San Andres Mountains to the east. Our research is conducted in the vicinity of a large experimental array deployed and operated by the Systems Ecology Lab (SEL) at the University of Texas at El Paso for studying desert vegetation lifecycles and soil-vegetation-atmosphere gas exchanges. Samples are collected at the north-eastern edge of this experimental array. The Creosote (*Larrea tridentata*) and Honey Mesquite (*Prosopis glandulosa*) were selected as the representative taxa of the study site, as they have become the two dominant species within the study area.

3. SAMPLE COLLECTION

Every two weeks three types of samples will be collected at the two sites within the study area. The following three types of samples are collected: any precipitation that has occurred following the last collection, plant stem samples from the Honey Mesquite and Creosote Shrub in each site, and soil samples taken at 10- and 20-centimeters depth at each site.

2.1 Precipitation Samples

3.1.1 Locate the rainfall collector at or around 32°35'0.64"N, 106°37'55.25"W

3.1.2 Taking a precipitation sample:

3.1.2.1 Carefully remove any rocks and soil at the base of the rainfall collector until the yellow lid of the clear container is revealed

3.1.2.2 Remove yellow lid to access small plastic centrifuge tube with blue lid

3.1.2.3 Remove blue lid

3.1.2.4 Replace with new centrifuge tube partially filled with mineral oil

3.1.2.5 Place blue lid of new centrifuge tube onto the tube with precipitation sample

3.1.2.6 Parafilm the centrifuge tube

3.1.2.7 Label the bottle with collection location, date, and time

3.1.2.8 Place the centrifuge vial into a zip-lock bag

3.1.2.9 Place the vial/bag into a cooler with icepacks

3.1.3 Repeat this process on each collection date following a precipitation event

3.1.4 Storing the sample in the laboratory:

3.1.4.1 Immediately place the sample into the refrigerator upon return from the field

2.2 Vegetation Stem Samples

3.2.1 Locate one of the study sites (Channel Area or Flat Area)

3.2.2 Identify one of the plants (Mesquite or Creosote)

3.2.3 Taking a stem sample:

3.2.3.1 Identify a healthy branch

3.2.3.1.1 Identify a twig with a diameter from 0.2 to 0.5 centimeters

3.2.3.1.2 Use gardening shears to cut the identified twig from branch

3.2.3.1.3 Cut twig into a piece that is 2 to 5 centimeters in length

3.2.3.1.4 Wrap the twig directly in parafilm

3.2.3.2 Repeat this process to collect 1 to 3 stems from each plant

3.2.3.3 Place wrapped twigs in zip-lock bag

3.2.3.4 Label the bag with each of the following:

3.2.3.4.1 Plant Type (M = Mesquite; C= Creosote)

3.2.3.4.2 Location (FA= Flat Area; CA= Channel Area)

3.2.3.4.3 Plant Number (1 or 2)

3.2.3.4.4 Collection Date

3.2.3.5 Place the bag into a cooler with icepacks

3.2.4 Repeat this process to collect from two Mesquites and two Creosotes from each of the study sites (a total of four Mesquites and four Creosotes)

3.2.5 Storing the samples in the laboratory:

3.2.5.1 Immediately place the sample into the refrigerator upon return from the field

2.3 Soil Samples

3.3.1 Locate an area of open soil that is between the two Mesquites and two Creosotes that were identified for one of the study sites (Channel Area or Flat Area)

3.3.2 Taking a soil sample:

3.1.2.1 Use a shovel to dig a small soil pit approximately 10 centimeters deep

3.1.2.2 Collect enough soil to fill a 4 oz glass sampling jar

3.1.2.2.1 Parafilm the jar

3.1.2.2.2 Label the jar with collection location, date, and depth

3.1.2.2.3 Place the jar into a cooler with icepacks

3.1.2.3 Continue digging into the pit until approximately 20 centimeters deep

3.1.2.4 Collect enough soil to fill a 4 oz glass sampling jar

3.1.2.4.1 Parafilm the jar

3.1.2.4.2 Label the jar with collection location, date, and depth

3.1.2.4.3 Place the jar into a cooler with icepacks

3.3.3 Repeat this process for the other site within the study area

3.3.4 Storing the samples in the laboratory:

3.3.4.1 Immediately place the sample into the refrigerator upon return from the field

APPENDIX B: PROTOCOL FOR ANALYZING STEM AND SOIL SAMPLES ON THE PICARRO L2130-I ANALYZER WITH AN INDUCTION MODULE

Hayden E. Thompson[1]

[1]Department of Geological Sciences, University of Texas at El Paso, El Paso, TX 79968, USA

1. SUMMARY

This appendix describes the general protocol that was used in analyzing soil and vegetation stem samples on the Picarro L2130-i Cavity Ring-Down Spectrometer assembled with an Induction Module (IM-CRDS). It provides our procedure for running blanks, isotopic standards, soil samples, and stem samples in the Ecohydrology Lab at the University of Texas at El Paso. All isotopic standards, soil, and stem samples are stored in a refrigerator in the lab until analysis.

2. PICARRO EQUIPTMENT

2.1 L2130-i Isotope and Gas Concentration Analyzer

2.2 External Vacuum Pump

2.3 Induction Module

3. MATERIALS FOR RUNNING STANDARDS AND SAMPLES

3.1 Syringes (10 μL; one for each standard)

3.2 Glass vials (4 mL with caps and septa)

3.3 Water standards (Zero, Mid, and Depleted)

3.4 Glass microfiber filter paper

3.5 Tri-fold metal envelope sample holders

3.6 Metal tube sample holders (3.5 mm)

3.7 Quartz wool

3.8 Hole punch

3.9 Tweezers

4. PREPARING TO ANALYZE SAMPLES / RUNNING BLANKS

4.1 Set up the analyzer and external vacuum pump by referring to the L2130-I Installation User's Manual.

4.2 Turn on the external vacuum pump using the physical switch located on its side. Then, turn on the analyzer using the physical switch located on the back. Let the analyzer run on ambient air until it has stabilized. **Note:** The analyzer is stabilized when it switches from

measuring cavity pressure (torr) to measuring water concentration (H_2O ppm) on the Graphical User Interface (GUI).

4.3 Set up the Induction Module (IM), connecting it to a gas flow controller and the analyzer, as shown in the Induction Module – CRDS Setup User's Manual. Turn on the zero-air gas to ~2.5 psi and set the gas flow controller to ~155 SCCM. Turn on the IM using the physical switch located on the back. A green light at the front of the IM will turn on and flash.

4.4 Start the IM Coordinator by selecting the "Coordinator Launcher" icon on the Desktop of the computer. Select "IM CRDS" from the drop-down menu. A new window will open for the IM Coordinator. **Note:** The water concentration on the GUI must be at or below 250 ppm in order to safely run standards or samples. Blank samples can be run to help lower the water concentration within the cavity.

4.5 To run blanks, select 'Calibration – Lower Temperature' from the Recipe Selection dropdown menu pop-up in the IM Coordinator window. For Data Type, select 'Blank'. A new pop-up will appear asking you to purge and prepare your sample. Press OK and prepare a capped empty vial.

4.6 Once prompted by the IM Coordinator, insert the blank vial into the left side of the IM using the leaver on the right side to operate the door, and press OK to run. Make sure that the door is closed before running the blank. When the blank is finished running a pop-up will notify you on the GUI. Use the leaver to open the door and take out the empty vial. **Note:** You can continue to run blanks as many times as needed to lower water concentration to ~250 ppm.

5. RUNNING STANDARDS OR LIQUID SAMPLES

5.1 Check that the water concentration listed on the GUI is at or below 250 ppm and verify that the IM is connected to the zero-air gas (set at ~2.5 psi) and the gas flow controller (set at ~155 SCCM) before running any standards or samples. Make sure that the IM Coordinator is launched as described above in step 4.4.

5.2 Prepare the materials needed to run standards or liquid samples:

5.2.1 Vials and Caps: Prepare 2 to 4 glass vials by placing a septum inside the cap with the shiny side facing out. **Note:** Glass vials can be reused, but it is recommended that they are set aside immediately following a run to cool down. Septa can be reused up to 4 times by rotating the vial between each sample run so that you do not pierce the septum twice in the same place.

5.2.2 Filter Paper Dots: Prepare filter paper dots using a hole punch to cut out small round pieces of the filter paper. Set aside for use in the tri-fold metal envelope sample holders.

5.2.3 Tri-fold Metal Envelope Sample Holders: Separate multiple tri-fold metal strips from the pack along the perforated lines. To prep a strip for liquid samples, place a filter paper dot between the flap, lined up with the round outline in the center of the strip. Close the tri-fold metal envelope with the filter paper in-between the two flaps. Fold over the two small triangle flaps, holding the filter paper in place. Use tweezers to crimp the middle and ends of the envelope to ensure that it is flat. Lastly, bend one end of the envelope 90° to allow it to lay flat within the glass vial.

5.3 To run standards or liquid samples, select 'Calibration – Lower Temperature' or 'Calibration – Higher Temperature' from the Recipe Selection dropdown menu pop-up in the IM Coordinator window. **Note:** It is recommended to test both recipe temperatures for proper accuracy with a given sample.

5.4 For Data Type, select 'Sample'. A new pop-up will appear asking you to purge and prepare your sample. Press OK and prepare the sample as follows:

5.4.1 Using a syringe, measure out approximately 3 μL of one of the water standards, or other liquid sample.

5.4.2 Empty the syringe onto the filter paper dot through the small hole in the center of the metal sample holder envelope prepared earlier in step 5.2.3.

5.4.3 Place the prepared sample into the glass vial with the bent end at the bottom of the vial. Seal the vial as quickly as possible to prevent evaporation of water.

5.5 Once prompted by the IM Coordinator, insert the glass vial into the left side of the IM using the leaver on the right side to operate the door, and press OK to run. Make sure that the door is closed before running the sample. When it is finished running a pop-up will notify you on the GUI. Use the leaver to open the door and take out the empty vial.

6. RUNNING STEM SAMPLES

6.1 Check that the water concentration listed on the GUI is at or below 250 ppm and verify that the IM is connected to the zero-air gas (set at ~2.5 psi) and the gas flow controller (set at ~155 SCCM) before running any samples. Make sure that the IM Coordinator is launched as described above in step 4.4.

6.2 Prepare the materials needed to run stem samples.

6.2.1 Vials and Caps: Prepare 2 to 4 glass vials by placing a septum inside the cap with the shiny side facing out. **Note:** Glass vials can be reused, but it is recommended that they are set aside immediately following a run to cool down. Septa can be reused up to 4 times by rotating the vial between each sample run so that you do not pierce the septum twice in the same place.

6.2.2 Tri-fold Metal Envelope Sample Holders: Separate multiple tri-fold metal strips from the pack along the perforated lines. Set aside until ready to prepare the sample for running.

6.3 To run stem samples, select ‘Woody Stems’ from the Recipe Selection dropdown menu pop-up in the IM Coordinator window. **Note:** The recipe for ‘Woody Stems’ was used for creosote and mesquite samples in our laboratory. Other recipes can be used or created to better fit a specific sample type. Reference the IM-CRDS Setup User’s Manual for advice in creating unique sample recipes.

6.4 For Data Type, select ‘Sample’. A new pop-up will appear asking you to purge and prepare your sample. Press OK and prepare the sample as follows:

6.4.1 Cut a small, ~2mm piece from the vegetation stem that was collected for analysis. Place this small vegetation piece between the flaps of a metal envelope

sample holder. Try to place the stem within the round outline in the center of the strip. Close the tri-fold metal envelope with the stem in-between the two flaps. Fold over the two small triangle flaps, holding the stem sample in place. Use tweezers to crimp the middle and ends of the envelope to ensure that it is flat. Lastly, bend one end of the envelope 90° to allow it to lay flat within the glass vial.

6.4.2 Place the prepared sample into the glass vial with the bent end at the bottom of the vial. Seal the vial as quickly as possible to prevent evaporation of water.

6.5 Once prompted by the IM Coordinator, insert the glass vial into the left side of the IM using the leaver on the right side to operate the door, and press OK to run. Make sure that the door is closed before running the sample. When it is finished running a pop-up will notify you on the GUI. Use the leaver to open the door and take out the empty vial.

7. RUNNING SOIL SAMPLES

7.1 Check that the water concentration listed on the GUI is at or below 250 ppm and verify that the IM is connected to the zero-air gas (set at ~2.5 psi) and the gas flow controller (set at ~155 SCCM) before running any samples. Make sure that the IM Coordinator is launched as described above in step 4.4.

7.2 Prepare the materials needed to run soil samples.

7.2.1 Vials and Caps: Prepare 2 to 4 glass vials by placing a septum inside the cap with the shiny side facing out. **Note:** Glass vials can be reused, but it is recommended that they are set aside immediately following a run to cool down. Septa can be reused up to 4 times by rotating the vial between each sample run so that you do not pierce the septum twice in the same place.

7.2.2 Metal Tube Sample Holders: Prepare metal tube sample holders by stuffing one side of the tube with a balled-up piece of quartz wool. The amount of quartz wool used needs to be sufficient enough to hold soil within the tube. Set aside until ready to prepare the sample for running.

7.3 To run soil samples, select ‘Clay Loam’ from the Recipe Selection dropdown menu pop-up in the IM Coordinator window. **Note:** The recipe for ‘Clay Loam’ was used for soil samples collected for analysis from our study locations within the Northern Chihuahuan Desert. Other recipes can be used or created to better fit a specific sample type. Reference the IM-CRDS Setup User’s Manual for advice in creating unique sample recipes.

7.4 For Data Type, select ‘Sample’. A new pop-up will appear asking you to purge and prepare your sample. Press OK and prepare the sample as follows:

7.4.1 Pour or scoop soil into the open end of the metal tube sample holder until almost full. Use another balled-up piece of quartz wool to ‘cap’ the open end and enclose the soil within the tube.

7.4.2 Carefully place the filled and enclosed metal tube into a glass vial. Seal the vial as quickly as possible to prevent evaporation of water.

7.5 Once prompted by the IM Coordinator, insert the glass vial into the left side of the IM using the leaver on the right side to operate the door, and press OK to run. Make sure that the door is closed before running the sample. When it is finished running a pop-up will notify you on the GUI. Use the leaver to open the door and take out the empty vial.

8. SHUTDOWN PROCEDURE

8.1 Ensure that the water concentration listed on the GUI is at or below 100 ppm and all coordinators have been exited. **Note:** The water concentration must be low to ensure that the cavity is dry before shutting down.

8.2 Select ‘Shutdown’ from the left side of the GUI. Allow the machine to slowly shut the programs down and turn off.

8.3 Turn off the IM using the physical switch located on the back. The green light at the front of the IM will turn off.

8.4 Turn off the external vacuum pump using the physical switch located on its side. Then, turn off the zero-air gas. Lastly, turn off the analyzer using the physical switch located on the back.

Vita

Hayden Thompson was born in Albuquerque, New Mexico to Laura Volz and Randy Thompson. She grew up in Corrales, New Mexico and graduated from Cibola High School in May 2013. Later that year, Hayden started college at New Mexico State University (NMSU) in Las Cruces, New Mexico and, after a few undecided semesters, chose to focus on geology. As an undergraduate student, Hayden participated in undergraduate research with Dr. Nancy McMillian. She used laser-induced breakdown spectroscopy (LIBS) to identify mineral standards for zircon, apatite, and sphene to be used in future provenance research. Hayden received her Bachelor of Science in Geological Sciences, as well as a minor in Natural Resources Economics, in May 2017. The following year, Hayden was admitted into the Department of Geological Sciences at the University of Texas at El Paso (UTEP) where she pursued her Master of Science degree. For the majority of her time as a graduate student, Hayden worked as a Research Assistant in the Ecohydrology Laboratory, focused on collecting and analyzing samples for her thesis project. She also worked for a semester as a Teaching Assistant for Historical Geology. In the fall of 2020, Hayden was awarded Outstanding Graduate Student in Geology by the Department of Geological Sciences at UTEP. Hayden received her Master of Science in Geology in December 2020.

Contact Information: hayden.eleanor@outlook.com

This thesis was typed by Hayden Eleanor Thompson